Published in final edited form as:
Exp Neurol. 2014 November ; 261: 563–577. doi:10.1016/j.expneurol.2014.07.010.

Functional Correlates of Exaggerated Oscillatory Activity in Basal Ganglia Output in Hemiparkinsonian Rats

Elena Brazhnik, **Nikolay Novikov**, **Alex J. McCoy**, **Ana V. Cruz**, and **Judith R. Walters**
Neurophysiological Pharmacology Section, National Institute of Neurological Disorders and Stroke National Institutes of Health, Bethesda, MD20892-3702USA

Abstract

Exaggerated beta range (13–30 Hz) synchronized activity is observed in the basal ganglia of Parkinson's disease (PD) patients during implantation of deep brain stimulation electrodes and is thought to contribute to the motor symptoms of this disorder. To explore the translational potential of similar activity observed in a rat model of PD, local field potentials (LFP) and spiking activity in basal ganglia output were characterized in rats with unilateral dopamine cell lesion during a range of behaviors. A circular treadmill was used to assess activity during walking; hemiparkinsonian rats could maintain a steady gait when oriented ipsiversive to the lesioned hemisphere, but were less effective at walking when oriented contraversive to lesion. Dramatic increases in substantia nigra pars reticulata (SNpr) LFP oscillatory activity and spike-LFP synchronization were observed within the beta/low gamma range (12–40 Hz) in the lesioned hemisphere, relative to the non-lesioned hemisphere, with the dominant frequency of spike-LFP entrainment and LFP power varying with behavioral state. At 3 weeks post-lesion, the mean dominant entrainment frequency during ipsiversive treadmill walking and grooming was 34 Hz. Other behaviors were associated with lower mean entrainment frequencies: 27–28 Hz during alert non-walking and REM, 17 Hz during rest and 21 Hz during urethane anesthesia with sensory stimulation. SNpr spike-LFP entrainment frequency was stable during individual treadmill walking epochs, but increased gradually over weeks post-lesion. In contrast, SNpr LFP power in the 25–40 Hz range was greatest at the initiation of each walking epoch, and decreased during walking to stabilize by 6 min at 49% of initial values. Power was further modulated in conjunction with the 1.5 s stepping rhythm. Administration of L-dopa improved contraversive treadmill walking in correlation with a reduction in SNpr 25–40 Hz LFP power and spike synchronization in the dopamine cell lesioned hemisphere. These effects were reversed by the serotonergic 1A agonist, 8-OH-DPAT. While the prominent spike-LFP phase locking observed during ongoing motor activity in the hemiparkinsonian rats occurs at frequencies intriguingly higher than in PD patients, the synchronized activity in the SNpr of this animal model has much in common with

*Correspondence should be addressed to Judith R. Walters, Ph.D., Neurophysiological Pharmacology Section, NINDS, NIH, 35 Convent Drive, Building 35 Room 1C905, Bethesda, MD 20892-3702 USA waltersj@ninds.nih.gov Tel: 301-496-2067.

Financial disclosures: There are no financial disclosures or conflict of interest for any of the authors. This article has not been submitted elsewhere. All co-authors have seen and agree with the contents of the manuscript.

oscillatory activity recorded from the basal ganglia of the PD patients. Results support the potential of this model for providing insight into relationships between synchronization of basal ganglia output induced by loss of dopamine and motor symptoms in PD.

Keywords

Parkinson's disease; basal ganglia; substantia nigra pars reticulata; beta frequency; local field potentials; gait; motor cortex; dopamine; 6-hydroxydopamine; serotonin; oscillations

INTRODUCTION

Recordings of neuronal activity from the subthalamic nucleus (STN) and internal globus pallidus (GPi) of Parkinson's disease (PD) patients during implantation of deep brain stimulation electrodes show exaggerated synchronized and oscillatory activity in the beta frequency range (13–30 Hz) (Alonso-Frech et al., 2006;Brown, 2003;Brown et al., 2001;Kuhn et al., 2005;Levy et al., 2002;Priori et al., 2004). Evidence that this beta range oscillatory activity is reduced by L-dopa treatment in the STN and GPi of PD patients (Alonso-Frech et al., 2006;Brown, 2003;Brown et al., 2001;Levy et al., 2002;Priori et al., 2004) in conjunction with improvement in motor function (Brown and Williams, 2005;Kuhn et al., 2006;Weinberger et al., 2006) has led to considerable interest in the source of this activity and its role in the development of parkinsonian symptoms.

Animal models of PD also show increases in synchronized and oscillatory activity in the basal ganglia (Avila et al., 2010;Belluscio et al., 2013;Bergman et al., 1994;Brazhnik et al., 2012;Delaville et al., 2014;Kita and Kita, 2011a;Mallet et al., 2008b;Murer et al., 2002;Raz et al., 2001;Sharott et al., 2005;Tachibana et al., 2011;Tseng et al., 2001;Walters et al., 2007). Ideally, these models should be able to provide insight into how loss of dopamine triggers such dramatic changes in basal ganglia activity and whether firing patterns in specific frequency ranges are ultimately pathological, compensatory, or simply confounding. One caveat, however, is that the peak frequencies of abnormal oscillations observed in animal models of PD show substantial variability across species and behavioral states, prompting questions about whether the increased oscillatory activity evident in animal models is translationally relevant to the oscillatory activity thought to be pathological in human PD. For example, in dopamine-depleted non-human primates, dominant frequencies of oscillatory spiking activity recorded from the STN and GPi are typically bimodally distributed in the 3–15 Hz range (Gatev et al., 2006;Heimer et al., 2006;Leblois et al., 2007;Raz et al., 2000;Tachibana et al., 2011), lower than the 13–30 Hz peak frequencies noted most commonly in local field potential (LFP) recordings from alert PD patients (Alonso-Frech et al., 2006;Brown, 2003;Kuhn et al., 2009;Levy et al., 2002;Priori et al., 2004;Weinberger et al., 2006). Moreover, peak frequencies of exaggerated oscillatory activity are in the 30–35 Hz range in LFP recordings from basal ganglia output nuclei in hemiparkinsonian rats during treadmill walking (Avila et al., 2010;Brazhnik et al., 2012), while studies in urethane-anesthetized hemiparkinsonian rats report synchronization in the 1 Hz range during deep anesthesia (Tseng et al., 2001;Walters et al., 2007) and in the 20 Hz range during states of global activation (Mallet et al., 2008a;Mallet et al., 2008b;Moran et

al., 2011). On the other hand, recordings from PD patients also show some variability in peak frequency from patient to patient under seemingly similar recording conditions, prompting questions about whether the specific frequency at which basal ganglia output becomes synchronized is critical, or even relevant, to the nature of the motor deficits in PD patients (Kuhn et al., 2009).

The present study sought to develop a more detailed description of relationships between oscillatory activity in basal ganglia output, behavioral state, and motor dysfunction in a rodent model of PD. Our goal was to determine whether the exaggerated oscillatory activity in the basal ganglia of the hemiparkinsonian rat model appears sufficiently relevant to the oscillations observed in the PD patient be helpful in elucidating how exaggerated oscillatory activity relates to the symptomology of PD. Chronic recordings of spike and LFP activity were performed in the substantia nigra pars reticulata (SNpr) in rats with unilateral 6-hydroxydopamine (6-OHDA)-induced dopamine cell lesion. Simultaneous recordings from the SNpr in the lesioned and non-lesioned hemispheres allowed assessment of the effect of dopamine cell lesion on basal ganglia output over a range of behavioral states. Dominant frequency and power of oscillatory neural activity, spike synchronization, and firing rate in the SNpr were analyzed over different time scales in conjunction with effects of L-dopa treatment on motor symptoms.

MATERIALS AND METHODS

All experimental procedures were conducted in accordance with the NIH Guide for Care and Use of Laboratory Animals and approved by the NINDS Animal Care and Use Committee. Every effort was made to minimize the number of animals used and their discomfort.

Subjects and behavioral training

Male Long-Evans rats (Taconic Farm, USA), weighing 250–300 g were housed with *ad libitum* access to food and water in environmentally controlled conditions with a reversed 12:12hr light:dark cycle (lights on at 6 PM). All rats (n=13) received unilateral dopamine cell lesions as described below. Rats with electrodes implanted bilaterally in the SNpr (n=9) were used for lesioned hemisphere vs non-lesioned hemisphere comparisons of LFP spectral power, spike-LFP synchronization and dominant entrainment frequency across behavioral states and for assessment of motor deficits during treadmill walking before and after administration of drugs (see below). An additional group of rats (n=4) with the electrodes unilaterally implanted in the SNpr of the DA-lesioned hemisphere were used to explore the relationship between the expression of synchronized activity in the high beta/low gamma frequency range (25–40 Hz) in the SNpr and the extent of motor deficits over the course of 2 hours following administration of a therapeutic dose of L-dopa. During the week before surgery, rats were handled daily and trained to walk on a circular treadmill (Avila et al., 2010). Training consisted of 3–5 daily sessions during which rats were encouraged to walk for 5–10 min in both clockwise and counterclockwise directions at variable speeds with rest periods between walking epochs. At the end of the training, the rats were able to walk steadily in both directions at the speed of 9 RPM. After unilateral dopamine cell lesion, the hemiparkinsonian rats could make reasonable progress on the circular treadmill if they were

oriented in the direction ipsiversive to the hemisphere with the dopamine cell lesion, with their affected paws on the outside of the circular path. They had significant difficulty walking in the direction contraversive to the lesion with their affected paws on the inside of the circular track.

Surgical Procedures

Unilateral lesion of the nigrostriatal pathway and implantation of electrodes for recording LFP and spikes and EMG electrodes were performed during the same surgery. Rats were anesthetized with 75 mg/kg ketamine (Ketaved, Vedco, St. Joseph, MO) and 0.5 mg/kg medetomidine HCl, administered i.p. (Dexdomitor, Pfizer Animal Health, New York, NY) and placed in a stereotaxic frame (David Kopf Instruments, Tujunga, CA, USA) with heads fixed with atraumatic earbars. The incision area was shaved and a long acting local anesthetic (1%, Polocaine, APP Pharmaceuticals, LLC, Schaumberg, IL) was injected along the intended incision lines. Ophthalmic ointment (Lacrilube, Akorn, Inc., Lake Forest, IL) was applied to prevent corneal dehydration and lidocaine gel was placed in the ear canals. A heating pad was used to maintain body temperature at 37°C. Small supplemental doses of ketamine were administered during the surgery as needed.

Unilateral lesion of the nigrostriatal pathway—Thirty minutes prior to intracerebral injections of 6-OHDA HBr (Sigma-Aldrich Co., St. Louis, MO) into the left medial forebrain bundle to destroy the dopaminergic nigrostriatal pathway, desmethylimipramine HCl (15 mg/kg, i.p.) (Sigma-Aldrich Co.) was administered to protect noradrenergic neurons. A hole was drilled in the skull at 4.4 mm anterior to the lambdoid suture, 1.2 mm lateral to sagittal suture. Six μg of 6-OHDA HBr in 3 μl of 0.9% saline with 0.01% ascorbic acid were infused via a 27 gauge stainless steel cannula into the medial forebrain bundle (8.3 mm ventral to the skull surface) at a rate of 1 μl/min over 3 min via a syringe pump (Harvard Apparatus, Holliston, MA, USA). The cannula was left at the target site for 3 min after the infusion was completed. The efficacy of the dopaminergic lesion was assessed using the stepping test procedure at 5–7 days after the lesion (Olsson et al., 1995; Schallert and Tillerson, 1999). Rats were included in the study if they demonstrated a strong unilateral motor deficit (number of steps made by the contralateral limb <5% of steps made by the ipsilateral limbs) after the DA cell lesion.

Electrode Implantation—Holes were drilled in the skull over the target recording sites in the left and right hemispheres. Two electrode bundles were bilaterally implanted into the SNpr at coordinates: +3.2 mm anterior to the lambdoid suture, 2.2 mm lateral from the sagittal suture and 8.0 mm ventral from the skull surface. Bundles were secured to the skull with screws and dental cement (Ortho-Jet Liquid, Lang Dental Mfg. Co., Inc, Wheeling, IL) and ground wires from each set of electrodes were wrapped around a screw located above the cerebellum. Two electrode configurations were used for these experiments: bundles, consisting of 8 stainless steel teflon-insulated microwires plus an additional 9th wire with no insulation for ~1 mm on the recording tip serving as a local reference, and arrays, consisting of 9 stainless steel microwires arranged in a 3×3 matrix with 200 μm between wires with the 9th reference wire at one corner of the array for recording from the larger area in the SNpr (NB Labs, Denison, TX, USA). Electrodes had impedances of ~0.6 MΩ, measured in

physiological saline at 135 Hz, 9th wires had impedances of ~0.2–0.3 MΩ. All rats were also chronically implanted with bipolar EMG electrodes consisting of two stainless steel wires coated with Teflon (Cooner Wire, Chatsworth, CA). EMG electrodes were inserted into the left and right scapular head of the deltoid and secured to the muscle by sutures. After completion of surgeries, ketofluid was given subcutaneously (s.c.), and atipamezole HCl (0.3 mg/kg, s.c.; Antisedan, Pfizer Animal Health, New York, NY) was administered to reverse the sedative effect of medetomidine. Rats were retrained on the rotating treadmill on the 5th postoperative day.

Electrophysiological recordings

Extracellular multiunit and LFP recordings were obtained from the SNpr ipsilateral and contralateral to the nigrastriatal dopamine cell lesion (n=9). Recording sessions started on day 7 post-surgery and were conducted weekly for 5–8 weeks. Sessions consisted of two walking epochs (5–10 min each) and two rest epochs (5–10 min each). Recordings were typically made during ipsiversive walking in the treadmill at rotation speed of 9 RPM, which was compatible with a slow walking pace for the rat. In addition to walking in the direction ipsiversive to the lesioned hemisphere, data were collected during 5 additional behavioral states: episodes of spontaneous grooming, attentive rest (epochs during ongoing auditory stimulation, when rats were alert and not initiating movements other than whisking), inattentive rest (periods of rest when rats were not whisking or looking around but with eyes open), paradoxical sleep (REM, periods of sleep with twitching limbs or whisking, 2 rats) and under urethane anesthesia (1 g/kg, i.p.) with mild sensory stimulation (light stroking) on the last day of the recordings.

Data for comparisons between lesioned and non-lesioned hemispheres were obtained before and after drug administration at day 21–23 post lesion while rats were walking in the direction ipsiversive to the lesioned hemisphere. To assess motor deficits and the effects of drug treatment on gait, data were also collected when rats were walking in the direction contraversive to the lesioned hemisphere. For these studies, a range of treadmill speeds was used.

Extracellular spike trains, LFPs, and bipolar EMGs were recorded using Plexon Inc. (Dallas, TX) and Spike2 (Cambridge Electronic Design, CED, Cambridge, UK) systems. Spikes and LFPs were referenced to the 9th wire in the SNpr from the same bundle or array. Sampling rates were 40 kHz for spikes and 1 kHz for LFPs and EMG. Action potentials were amplified (10,000X) and band-pass filtered (0.15–9 kHz). LFPs were amplified (1000X) and band-pass filtered (3–170 Hz) and EMGs were amplified (1000X) and band-pass filtered (0.1–1 kHz). Discriminated spike signals, LFPs and EMG recordings were digitized, stored and analyzed using Spike2 data acquisition and analysis software (CED).

Drug Administration

Drugs (Sigma-Aldrich Co. St. Louise, MO) were dissolved in sterile saline and injected i.p. On day 21–23 post-lesion, rats were administered a therapeutic dose of L-dopa (5 mg/kg, supplemented with 15 mg/kg benserazide HCl). One group of rats were administered the D2 receptor antagonist eticlopride (0.2 mg/kg) 40–60 min after administration of L-dopa. Other

rats received the serotonin (5HT) 1A specific receptor agonist (8-OH-DPAT, 0.2 mg/kg) 40 min after L-dopa, and after a subsequent 20 min, the 5HT-1A specific receptor antagonist (WAY-100635, 0.3 mg/kg).

Data Analysis

Identification of the epochs for analysis—Periods of LFP and spike recordings free of major artifacts were selected for analysis. EMG activity, direct observation, and videotaped motor behavior were used for selection of epochs representing different behavioral states. For spike-triggered waveform averages (STWA) and LFP power, epochs of 100 s were used during attentive rest (alert non-walking), walking, REM sleep and urethane anesthesia, and 40–100 s epochs were used for inattentive rest and grooming. Epochs of 100 s were used to assess mean firing rates during walking. Walking epochs represent data taken when rats were walking on the circular treadmill in the direction ipsiversive to the lesioned hemisphere, unless otherwise indicated.

Spectral analysis of LFPs—LFP recordings were smoothed to 250 Hz and LFP power was analyzed by fast Fourier transform (FFT) with a frequency resolution of 1 Hz. Total power in 12–25 Hz (low beta) and 25–40 Hz (high beta/low gamma) and 45–60 Hz (gamma) frequency ranges was calculated using a Spike2 script. LFP power from two electrodes per bundle and two epochs for each behavioral condition were averaged, normalized by total power within the 70–100 Hz range, and presented as the ratio of power in lesioned hemisphere versus power in non-lesioned hemisphere. In the experiments with L-dopa treatment and consecutive administration of other drugs, the alterations in total LFP spectral power in high beta/low gamma frequency range were evaluated before and after drug treatments while the rat was walking in the circular treadmill.

To visualize spectral power changes over time for the selected epochs, time-frequency wavelet spectra were constructed using continuous wavelet transforms. The Morlet wavelet was applied to the LFPs using 128 frequency scales and a time resolution of approximately 750 ms (Time-Frequency Toolbox, http:tftb.nongnu.org).

EMG-LFP amplitude modulation—Relationships between EMG from the shoulder muscle (scapular head of the deltoid) contralateral to the lesion and simultaneously recorded LFP were examined in 11 rats to assess amplitude modulation of 25–40 Hz SNpr oscillations in conjunction with motor activity. LFP recordings were band pass-filtered at 25–40 Hz, EMG and LFP signals were rectified and smoothed (time constant of 0.04 s). Waveform cross-correlations were calculated for four LFP channels per rat in the lesioned hemisphere paired with the contralateral EMG channel, using the EMG channel as the reference. Results were then averaged for each rat and then across the rats. Modulation in 25–40 Hz LFP amplitude was considered significantly correlated with EMG activity during treadmill walking if the peak and trough of the cross correlation centered around time 0 exceeded 3 standard deviations (SD) of the mean waveform amplitude from the −2.0 to −1.5 and 1.5 to 2.0 s segments of the cross correlation. A further comparison of relative changes in 25–40 Hz SNpr LFP power and contralateral EMG over the first 6 min of walking epochs was performed. Instantaneous RMS was obtained for 6 consequtive 1 min intervals of

rectified EMG activity. SNpr LFP power from 4 channels over the same intervals was averaged per rat for 8 rats and the averaged across rats. A separate group of 6 non-lesioned rats were used for control data. The Pearson correlation coefficient was computed to assess change over time of SNpr LFP vs rectified EMG RMS.

Cell sorting—For rate and spike-triggered waveform average (STWA) peak-to-trough analysis, spikes were sorted offline using Spike2 algorithms and principal component analysis (PCA). To assess the effectiveness of the single cell sorting procedure, interspike interval histograms were generated and inspected to ensure that the first ms of the histogram, representing the refractory period, was free of spikes. For multiunit spike-triggered waveform averages, action potential waveforms on a given wire were discriminated as single units initially and then recombined to form a multiunit spike train typically consisting of 2–5 cells to reflect population activity.

SNpr spike-LFP synchronization—STWAs were used to assess the degree of phase-locking (i.e. synchronization or entrainment) of the spiking activity to LFP oscillations. STWAs were generated from two 100 s epochs of single or multiunit spike trains and simultaneous LFP recordings (except during rest when epochs varied from 40 to 100s). LFPs were smoothed to 500 Hz and band-pass filtered at 12–45 Hz. STWAs were generated from epochs of spike and LFP recordings from the lesioned and non-lesioned hemisphere over the range of behaviors and the STWA peak-to-trough amplitude around time 0 was obtained. To determine the significance of the peak-to-trough value as a measure of spike-LFP synchronization, additional STWAs were generated from the same spike train after the spike train interspike intervals were shuffled. Each shuffled spike train was used to create another STWA. This process was repeated 20 times to obtain a set of 20 peak-to-trough amplitudes, which were averaged to provide a mean peak to trough amplitude and SD for the shuffled data.

To measure the extent of spike-LFP synchronization in a population of neurons, the ratio of the unshuffled spike train STWA peak-to-trough amplitude relative to the mean shuffled spike train STWA peak-to-trough amplitude was calculated. If there was no phase-locking in the unshuffled spike train, the ratio would be close to 1.

Another index of the extent of spike-LFP synchronization in a population of neurons calculated was the percentage of correlated neurons. This was obtained using only STWAs from spike trains sorted for single units. A spike train was considered to be significantly correlated with the LFP oscillation when the peak-to-trough amplitude of the unshuffled spike train STWA was greater than the mean ± 3 SD of the 20 shuffled spike train peak-to-trough values.

Dominant multiunit spike-LFP entrainment frequency—Data from STWAs generated from multiunit spike trains was used to to estimate the frequency of the LFP oscillations to which the spike train was preferentially entrained. The STWA LFP oscillations triggered by the spikes from 4 multiunit trains per hemisphere over two 100 s epochs, or four 30 s epochs per behavioral state, were obtained. The dominant multiunit entrainment frequency was calculated as the reciprocal of the time between the successive

peaks in the STWA closest to zero and averaged in order to identify the dominant entrainment frequency of LFP oscillatory activity in the 12–45 Hz frequency range for each rat and each behavioral state. For a subset of neurons, dominant spike-LFP entrainment frequencies were also obtained from STWA analysis of single unit data and from peak frequencies obtained from examination of the power spectra of the STWA waveforms (Fries et al., 2001) to confirm accuracy of the multiunit approach.

Effect of drug administration—STWAs were generated from 100 s single unit spike trains using LFPs filtered in the 25–40 Hz. Data were taken from epochs during treadmill walking before and following the administration of L-dopa and after consecutive administration of the 5HT-1A receptor agonist 8-OH-DPAT and 5HT-1A receptor antagonist WAY-1000635 at day 21–23 post- lesion to obtain the percentage of SNpr neurons significantly phase-locked to the LFP activity and ratios of unshuffled to shuffled STWA peak-to-trough amplitudes. In addition, firing rates of the SNpr cells were determined to compare mean rate changes following L-dopa treatment and after administration of the 5HT1A receptor agonist and antagonist.

Motor performance—Motor activity was monitored online and videotaped for offline review. To quantify the motor performance of the intact and DA-depleted rats during epochs of walking in a circular treadmill, the number of steps made by each of the hindpaws, i.e. the paws toward the inside and the outside of the circular treadmill track, were counted during two 30 s epochs of walking in each direction. The count was taken at four treadmill rotation speeds ranging from 5 to 9 RPM. The ratio of steps made by the inside paw relative to steps made by the outside paw was calculated and averaged across the rotation speeds.

Statistics—Data are reported as mean ± standard error of the mean (SEM). Unless stated otherwise, statistical significance was evaluated with 1-way or 2-way repeated measures analysis of variance (RM ANOVA) with Student Newman-Keuls *post hoc* comparison. If normality failed, Friedman RM ANOVA with Dunnett's *post hoc* comparison was used. Statistical analysis was performed using Sigma Plot software (SyStat Software, San Jose, CA). The criterion for significance was $p<0.05$.

Histology and immunochemistry

After recordings were completed, rats were initially lightly anesthetized with urethane (1.0 g/kg, i.p.) for recordings during sensory stimulation, and subsequently more deeply anesthetized (an additional 0.6 g/kg urethane, i.p.) and recording sites were marked by passing a positive current of 10 μA for 10 s via 2–3 microwires. Rats were perfused intracardially with 200 mL cold saline followed by 200 mL 4% paraformaldehyde in phosphate buffer solution (PBS). Brains were post-fixed in paraformaldehyde solution overnight and then immersed in 10% sucrose in phosphate buffered saline (0.1 M, pH 7.4). Coronal sections of 35 μm were collected in PBS. Sections for electrode placement verification were mounted on glass slides and stained with cresyl violet and 5% potassium ferricyanide/9% HCl to reveal the iron deposited at the electrode tips.

To assess the loss of dopaminergic neurons in the SNpc, a standard immunohistochemical protocol was used for staining tyrosine hydroxylase (TH) in freely floating sections. Briefly, brain sections were washed 3 times in PBS (0.01 M, pH 7.4) prior to incubation with rabbit polyclonal anti-TH antibody (1:200 dilution; Pel-Freez Biologicals, Rogers, AR) for 12–18 hr at room temperature, with moderate agitation. Sections were rinsed 3 times in PBS and incubated with secondary antibody biotinylated anti-rabbit IgG (1: 200 dilution; Vector Laboratories, Burlingame, CA). After 1 h of incubation, sections were rinsed three times in PBS and incubated with avidin-biotin-perioxidase complex (ABC kit; Vector Laboratories) for 60 min, then rinsed in 50 mM Tris (pH 7.4) and reacted with 0.05% 3,3'-diaminobenzidine tetrahydrochloride and 0.01% H_2O_2 (DAB kit, Vector Laboratories) for 2–10 min until intense staining emerged. Sections were washed in 50 mM Tris then mounted on slides, dehydrated, and prepared for light microscopy.

The extent of dopamine cell degeneration was assessed by examination and digitization of the image under the light microscope obtained with wide-field optics allowing simultaneous capture of both lesioned and non-lesioned hemispheres. The optical density values of TH fibers and neurons in the substantia nigra were measured (using ImageJ software, NIH) in anterior, middle, and posterior sections of the substantia nigra in the lesioned hemisphere and compared with density in homologous regions in the non-lesioned hemisphere. TH density in substantia nigra from the lesioned hemisphere was reduced by more than 88% (averaging 96.0±1.5% reduction) relative to that in the non-lesioned hemisphere.

Results

Behavioral State-Dependent Changes in SNpr LFP Activity and Synchronized Spiking after Dopamine Cell Lesion

Chronic recordings from electrodes implanted bilaterally in the substantia nigra pars reticulata (SNpr) confirmed previous observations (Avila et al., 2010; Brazhnik et al., 2012) of increases in oscillatory LFP activity in this nucleus during rest and treadmill walking after unilateral 6-OHDA-induced dopamine cell lesion. As shown in wavelet-based scalograms and FFT-based power spectra (Fig. 1A, left and right panels), SNpr LFP activity in the dopamine-deprived hemisphere was dramatically different from SNpr LFP activity recorded simultaneously in the contralateral intact hemisphere over a range of behavioral states, from alert non-walking, treadmill walking and grooming to inattentive rest, rapid eye movement (REM) sleep and during urethane anesthesia with sensory stimulation (urethane+SS). The scalograms and LFP power spectra further indicate that both peak frequency and power of beta/low gamma LFP oscillations in the lesioned hemisphere vary in subtle as well as substantial ways depending on the behavioral state of the rat.

SNpr LFP power over a range of behaviors—To examine the effects of different behavioral states on changes in SNpr LFP power after dopamine cell lesion, the relationship between SNpr LFP power in the lesioned vs intact hemisphere was examined over three frequency ranges: low beta (12–25 Hz), high beta/low gamma (25–40 Hz), and gamma (45–60 Hz). Inattentive rest, alert non-walking, grooming, and treadmill walking epochs were

recorded at day 21–23 post lesion and urethane+SS epochs were recorded at day 40–50 post lesion (Fig. 1B).

In the low beta range (12–25 Hz), no significant differences in SNpr LFP power were observed between the dopamine cell lesioned and non-lesioned hemispheres for alert non-walking, ipsiversive treadmill walking, and grooming behaviors. Lesioned/intact power ratios for these behaviors were in the range of 1.1–1.4. During epochs of inattentive rest and urethane+SS, however, LFP SNpr power was significantly greater in the lesioned hemisphere in this range (rest, $p<0.001$, n=9; urethane, $p<0.003$, n=8) with lesioned/intact LFP power ratios of 2.1±0.4 and 2.9±0.4 respectively, for these behaviors (Fig. 1B).

In contrast, in the 25–40 Hz high beta/low gamma frequency range, LFP power during grooming, alert non-walking, and walking was significantly greater in the lesioned hemisphere than in the non-lesioned hemisphere ($p<0.001$, n=9, Fig. 1B), with power in the lesioned hemisphere increased 4 – 6 fold relative to the non-lesioned hemisphere. Epochs recorded during urethane+SS in this frequency range showed lesioned/intact LFP power ratios of ~2, as observed in the lower 12–25 Hz range, reflecting the fact evident in the wavelet scalogram and LFP power spectra in Fig. 1A, that increases in LFP power during this anesthetized state overlap the low beta/high beta ranges.

Ratios of intact/lesioned LFP power in gamma frequency range (45–60 Hz) were ~1 for all behaviors, with no significant differences between hemispheres over specific behavioral states ($p>0.05$, 1-way RM ANOVA).

Also shown in Fig. 1A is one of two epochs during which SNpr LFP activity was recorded while the rats showed classical signs of REM sleep (i.e. twitching limbs, or whisking). As represented by the wavelet based spectrogram (Fig. 1A, left panel) and FTP-based power spectrum (Fig. 1A, right panel), the LFP oscillatory activity in the 20–35 Hz range was quite striking in the lesioned hemisphere during these epochs.

Dominant entrainment frequency of spike/LFP synchronization over a range of behaviors—Simultaneous recordings in the intact and lesioned hemispheres showed that phase-locking of SNpr spiking activity to SNpr LFP oscillations filtered in the 12–45 Hz range was dramatically greater in the lesioned hemisphere, relative to the non-lesioned hemisphere, during all behavioral states, as shown in Fig. 1C (2-way RM ANOVA, $p<0.001$). The unshuffled/shuffled peak-to-trough amplitude ratios were 3–4 times higher in the lesioned hemisphere than in the non-lesioned hemisphere for all states (Fig. 1C, see 7A for example of STWA from the lesioned hemisphere). There was no significant difference between the behavioral states (1-way RM ANOVA, $p=0.46$). These observations show that increases in high beta/low gamma oscillatory activity in the SNpr LFPs after dopamine cell lesion are linked to significant increases in synchronized spiking in the SNpr neuronal population.

To examine how the specific frequency of the spike-LFP phase-locking varies with behavioral state, we determined, as shown in Fig. 1D, the average dominant entrainment frequencies of the phase-locked activity for the same series of states across rats. The

entrainment frequency of the STWA, calculated as the reciprocal of the time between successive peaks in the STWA closest to zero, was typically similar to the peak frequency observed in the simultaneously recorded LFP power spectra. Fig. 2 shows the distribution of the dominant entrainment frequencies for individual rats for alert and treadmilll walking states at 14–23 days post-lesion and during urethane+SS at 40–50 days post-lesion. The average entrainment frequency observed during the intense stereotyped movements associated with episodes of grooming was strikingly similar to that observed during treadmill walking (walking 34.2±0.3 Hz, and grooming: 34.1±0.6 Hz, $p=0.39$). Notably, these two behaviors were characterized by significantly higher entrainment frequencies than those observed during alert non-walking (27.7±0.5 Hz) (1-way RM ANOVA, $p<0.001$, $n=9$). The dominant LFP frequencies that emerged in the two REM epochs were similar to frequencies observed during the alert non-walking state. During inattentive rest, the STWAs showed prominent spike-LFP phase-locking relationships with mean frequencies of 16.9±0.7 Hz in the low beta frequency range.

The dominant spike-LFP entrainment frequencies that emerged in recordings under urethane +SS showed substantial variability across rats (see Fig. 2) but the mean value (20.8±1.1 Hz, $n=8$) was significantly lower than the dominant entrainment frequencies observed during walking, grooming and alert non-walking in the awake rats. The range of frequencies observed during urethane+SS is similar to that reported in studies on urethane anesthetized rats during periods of cortical desynchronization, often referred to as “global activation” and frequently induced, as in the present study, by sensory stimulation (Mallet et al., 2008a;Mallet et al., 2008b;Moran et al., 2011). Note that the dominant entrainment frequencies for treadmill walking and alert non-walking were quite consistent with only modest variation between rats (Fig. 2).

Collectively, the results indicate that transition from more active states, such as alert non-walking, treadmill walking and grooming to inattentive rest and anesthesia+SS is associated with shifts in the dominant frequencies of LFP oscillatory activity and spike-LFP synchronization from higher to lower frequency ranges (Fig. 1D). These observations suggest that circuits driving the synchronization of SNpr spiking in the lesioned hemisphere are quite flexible and behaviorally relevant.

Time-Dependent Changes in SNpr LFP Power and Frequency after Dopamine Cell Lesion

LFP power and dominant frequency over 10 min walking epochs—To explore correlates of increased LFP activity in basal ganglia output with behavioral state, the variability of high beta/low gamma power during treadmill walking was assessed over a range of time intervals. Fig. 3A and 3B show data from a typical treadmill walking epoch in a hemiparkinsonian rat, demonstrating a distinct reduction in high beta/low gamma activity over the course of first few minutes of an ipsiversive walking episode. Data represent epochs of walking at the standard treadmill speed of 9 RPM, corresponding to a slow stepping speed of ~40 steps per minute, averaging one step every 1.5 sec.

SNpr LFP power in the 25–40 Hz range was greatest at walking onset and diminished gradually until the 4–5th min as indicated in the wavelet-based scalogram (Fig. 3A). After this initial reduction, the high beta/low gamma power remained relatively constant at ~50%

of its initial power during the remainder of the 11 min walking period. Fig. 3C shows that the mean total SNpr LFP power in the lesioned hemisphere in the 6th min was significantly reduced from that in the 1st min of continuous walking in rats studied 18–23 days post lesion (2-way RM ANOVA, $p<0.001$; n=9). In contrast, total SNpr LFP power in the non-lesioned hemisphere for the same frequency range during the same walking epochs did not show any significant difference between the 1st and 6th min of continuous walking in the treadmill, and was significantly lower than LFP power in the lesioned hemisphere ($p<0.006$). In line with this, Fig. 3D demonstrates that LFP beta power was consistently greater at the onset of each walking episode in the dopamine cell lesioned hemisphere, during multiple consecutive 2.5 min episodes of treadmill walking over a range of treadmill speeds, with consistent reduction in power over time. Interestingly, decreases in SNpr LFP 25–40 Hz power during the first 6 min of walking was reflected in the variability in EMG activity as assessed by examining the cross correlation between EMG RMS and LFP 25–40 Hz power averaged over 1 min intervals for 6 min after the initiation of walking (data not shown). Decreases in both measures were evident over the 6 min walking epoch and were significantly correlated (Pearson correlation, $r=0.99$, $p<.001$, n = 8 rats). Similar data from a separate set of control rats during treadmill walking showed no significant correlation ($r=-0.22$, $p>0.5$, n=6).

Unlike LFP power, the dominant entrainment frequency of the high beta/low gamma LFP oscillations remained stable during the walking epoch shown in Fig. 3A and 3E. No significant difference was observed between the 1^{st} and 6^{th} min of continuous treadmill walking (1-way RM ANOVA, p=0.9, n=9, data not shown). Similarly, an increase of treadmill rotation speed produced no significant variation in the dominant entrainment frequency within the high beta/low gamma range (1-way RM ANOVA; p=0.75; n=9, data not shown).

LFP power and dominant entrainment frequency between 7 and 40–50 days post lesion—To further examine the stability of the increased SNpr LFP high beta/low gamma total power over a period of days to weeks after dopamine cell lesion, LFP recordings from the same electrodes were analyzed at days 7 and 21 and at day 40–50 post lesion for the epochs of treadmill walking. Although individual rats showed some variation in LFP power over time, there was no significant change in mean 25–40 Hz SNpr LFP power within the lesioned hemisphere over same post-lesion period during treadmill walking as shown on Fig. 3F (p=0.24, n=8). Thus, the results show that SNpr LFP power in the 25–40 Hz frequency range remains consistently enhanced in the SNpr LFPs of the lesioned hemisphere more than 4–8 weeks after dopamine cell lesion, although expression is reduced over time during the course of individual treadmill walking epochs.

In contrast to the stability in the exaggerated SNpr LFP power in the 25–40 Hz frequency range during treadmill walking over time post lesion, the dominant multiunit spike-LFP entrainment frequency in this range exhibited a gradual shift to higher values during the same period (Fig. 3G). The mean dominant frequency in 25–40 Hz LFP activity changed from 30.8±0.4 Hz at 7 days post-lesion to 34.2±0.3 Hz at 21 days post-lesion and reached the higher value of 37.0±0.4 Hz at 40–50 days after dopamine cell lesion. The significant difference in mean entrainment frequency over the 3 post-lesion time intervals was

confirmed by 1-way RM ANOVA ($p<0.002$). These results are consistent with previously reported data showing significant increases in peak LFP power in the 25–40 Hz range over a period of weeks in the SNpr and motor cortex of the lesioned hemisphere in the hemiparkinsonian rat (Brazhnik et al., 2012).

LFP amplitude modulation over the stepping cycle during treadmill walking— To determine whether expression of the high beta/low gamma oscillatory activity in basal ganglia output varies with changes in motor activity on time scales relevant to the rats' stepping rhythm, we asked whether the amplitude of the 25–40 Hz LFP activity varies with the amplitude of the EMG recorded in the forelimb contralateral to the lesioned hemisphere during treadmill walking. The 1.5 sec stepping rhythm observed when these rats walked in the circular treadmill at the standard 9 RPM speed is reflected in the rectified EMG trace by a series of concurrent peaks. (Fig. 4C). Alterations in beta range LFP power are also evident within this time frame, as indicated by Fig. 4A and B. As shown by the LFP-EMG waveform cross-correlation in Fig. 4D, the amplitude modulation of the SNpr 25–40 Hz LFP in the dopamine cell-lesioned hemisphere was significantly correlated with the modulation of EMG during stepping. Thus, the magnitude of 25–40 Hz range LFP power in the SNpr is modulated by stepping during treadmill walking. This analysis supports the view that phasic increases and decreases in SNpr LFP power in the 25–40 Hz range occur on a time scale relevant to the sequence of movements of the affected forelimb performed by the rat as it walks on the treadmill. However, it was not possible with the present data to determine whether a particular phase of the correlated 1.5 s LFP-EMG amplitude oscillation reflects movement preparation or execution.

Correlation between L-dopa-induced Reduction in SNpr LFP Power and Improvement in Treadmill Walking after Dopamine Cell Lesion

We next examined how L-dopa administration's ability to reduce 25–40 Hz SNpr LFP activity in the dopamine cell-lesioned hemisphere (Avila et al., 2010;Brazhnik et al., 2012) correlates with improvement of motor deficits as assessed with the use of the circular treadmill. After dopamine cell lesion, differences in gait were noted depending on which direction the rats were walking on the circular treadmill. Rats with left hemisphere DA cell lesions showed greater difficulty walking on the treadmill at the target speed if their impaired limbs, contralateral to lesion, were on the inside of the circular path (contraversive walking; see the cartoon on the upper left, Fig. 5A). However, rats were able to walk steadily in opposite direction, when the impaired limbs were on the outside of the circular path (ipsiversive walking; see the cartoon on the upper right, Fig. 5B). Althought it remains possible that additional training in the treadmill might lead to improvement in contraversive walking, the deficits in contraversive walking were consistent over the course of the study.

To show that the increases in SNpr high beta/low gamma power were associated with deficits in treadmill walking in the hemiparkinsonian rat, we examined SNpr LFP activity before and after treatment with therapeutic doses of L-dopa (5 mg/kg). Treatment with L-dopa markedly reduced LFP power in the 25–40 Hz range in a manner significantly correlated with improvement in treadmill walking in the direction contraversive to the lesioned hemisphere, as shown on Fig. 5B. The mean ratio of LFP 25–40 Hz power during

treadmill walking after L-dopa treatment, relative to power before L-dopa treatment (baseline), and the mean ratio of inner vs. outer paw stepping (see Methods) were calculated every 20 min over a two hour period after the administration of L-dopa. Rats were walking in contraversive (Fig. 5C) and ipsiversive directions (Fig. 5G) at 5 RPM and 9 RPM, respectively; Fig. 5D shows a strong positive correlation between reduction in 25–40 Hz power and the ability to walk contraversive in the circular treadmill (Pearson correlation: $r=0.781$; $p<0.001$, $n=5$). Notably, L-dopa treatment did not affect ipsiversive treadmill walking (Pearson Correlation: $r=0.07$; $p=0.82$), as shown in Fig. 5H.

8-OH-DPAT-induced Reversal of L-dopa Effects on SNpr LFP Activity and Motor Deficits

To further explore the relationships between motor dysfunction, increases in SNpr LFP activity and loss of dopamine, we examined the ability of 8-OH-DPAT, a 5HT1A agonist, to reduce the effects of L-dopa administration on both contraversive treadmill walking and high beta/low gamma range oscillations in the SNpr in the hemiparkinsonian rat. Serotonergic neurons are thought to be involved in the conversion of L-dopa to dopamine and the release of dopamine in advanced PD in which there is a marked loss of dopamine neurons (Carta et al., 2007;Maeda et al., 2005;Navailles et al., 2010;Politis et al., 2014). Serotonergic 1A agonists can reduce dopamine release under these conditions as these agonists inhibit the activity of serotonergic neurons (Aghajanian et al., 1990;Kannari et al., 2001;Lindgren et al., 2010;Munoz et al., 2008).

As shown in Fig. 6A, C and D, administration of 8-OH-DPAT effectively reversed the effects of L-dopa in the dopamine cell lesioned hemisphere, reinstating both the high beta/low gamma power band in the SNpr LFP recordings during treadmill walking and the impairment of the rats' ability to walk in direction contraversive to the lesion, as reflected by reduction of the mean step ratio to 0.50±0.03 (Fig. 6D, right panel, $p<0.001$, $n=7$; 2-way RM ANOVA).

Notably, in the same rats, a second period of improved contraversive walking was observed together with a second reduction of beta oscillatory activity upon subsequent administration of WAY-100635, a 5HT1A antagonist (Martin et al., 1999). This antagonist reversed the effects of 8-OH-DPAT as shown in Fig. 6A and C, significantly reducing the LFP high beta/low gamma power ($p<0.001$) and improving treadmill walking in the direction contraversive to lesion, with a stepping ratio of 0.89±0.03, which was not significantly different from the ipsiversive direction ($p>0.5$, Fig 6E, right bar graph).

The effects of sequential administration of low dose L-dopa, 8-OH-DPAT and WAY-100635 were also examined in rats under urethane+SS anesthesia ($n=5$). As described above, mild sensory stimulation under urethane anesthesia induced steady and long lasting episodes of LFP beta range oscillations in the lesioned hemisphere. As seen with the awake rats, administration of L-dopa markedly reduced LFP range power in the SNpr of the dopamine cell lesioned hemisphere as shown by wavelet based scalograms in Fig. 6B and bar graph in Fig. 6C (right panel, $p<0.05$, 1-way RM ANOVA). Administration of 8-OH-DPAT reversed the effects of L-dopa and restored LFP beta range power in the SNpr to the values that were not different from baseline. Subsequent administration of WAY-100635 significantly reduced LFP beta power, as it did in awake rats ($p<0.02$, Fig. 6C). These

results show that serotonergic agents believed to modulate the release of dopamine have similar effects on the exaggerated LFP activity expressed in walking rats and in urethane-anesthetized rats, even though the LFP oscillations are expressed at different frequencies in the two conditions. Thus, mechanisms associated with increased activity in the 20 Hz range as well as the 30–35 Hz range appear comparably sensitive to alterations in dopamine receptor stimulation.

To compare the effect of 8-OH-DPAT with that of a dopamine antagonist with respect to the impairing ther rats' ability to walk contraversive to the lesion after L-dopa treatment, treadmill walking was also examined after acute administration of 0.2 mg/kg eticlopride, 40–60 min after administration of L-dopa. Blockade of dopamine receptors with eticlopride after L-dopa treatment has been shown to reinstate the increase in 25–40 Hz LFP power in the SNpr of the lesioned hemisphere (Brazhnik et al., 2012). This treatment is also associated with reinstatement of the impairment in treadmill walking in the direction contraversive to dopamine cell lesion as shown in the present study by mean step ratio in Fig. 6D (left bar graph). It is interesting to note that acute blockade of D2 dopamine receptors with eticlopride did not affect SNpr LFP activity in the non-lesioned hemisphere. There was no evidence of an increase in oscillatory activity in the beta frequency range in the non-lesioned hemisphere as treadmill walking became impaired after administration of eticlopride (data not shown).

SNpr spike synchronization and SNpr firing rates—To determine whether changes in synchronization of SNpr spiking activity and firing rate are affected in parallel with changes in beta power and behavior, the effects of sequential administration of L-dopa, 8-OH-DPAT and WAY-100635 on SNpr single unit spike-LFP relationships were examined in SNpr spike trains recorded from the lesioned and non-lesioned hemisphere. As illustrated in the example shown in Fig. 7A and averaged STWA-based peak-to-trough ratios shown in 7B, phase-locking of SNpr spikes with the LFP activity in the high beta/low gamma frequency range in the lesioned hemisphere during treadmill walking was reduced following administration of L-dopa, while subsequent administration of 8-OH-DPAT reversed the effect of L-dopa and restored coherent spike-LFP relationships. Administration of WAY-100635 effectively reduced synchronization of spiking with LFP activity in the SNpr, reversing the effect of 8-OH-DPAT on peak-to-trough ratios (31 single units, 7 rats). In contrast, neurons recorded in the non-lesioned hemisphere (25 single units, 7 rats) did not show notable synchronization of spiking with LFP, nor modulation of their STWA peak-to-trough ratios by these drugs. Similarly, as shown in 7C, the percentage of these neurons that were significantly phase-locked to the high beta/low gamma LFP in baseline (68%) and after 8-OH-DPAT (65%) in the SNpr in the lesioned hemisphere was substantially greater than in the non-lesioned hemisphere (4%, 8%, respectively).

Mean firing rates of these SNpr neurons were also significantly altered by this sequence of drugs. L-dopa induced a significant decrease in the lesioned hemisphere from 20.3±3.2 to 13.6±2.2 Hz; rates were restored to 18.2±3.2 Hz by 8-OH-DPAT and after WAY-100635, significantly reduced to 11.1±1.8 Hz (Friedman RM ANOVA, $p=0.02$). SNpr firing rates were not significantly affected in the simultaneously recorded non-lesioned hemisphere ($p=0.16$).

Collectively, these data show a correlation between changes in LFP power and spike synchronization in the dopamine cell lesioned hemisphere, and support the view that exaggerated LFP oscillations recorded in the SNpr reflects synchronized input to this region as well as synchronized output.

DISCUSSION

The present study explores the characteristics of the increases in oscillatory activity in the basal ganglia output in the hemiparkinsonian rat. Our goal was to assess the potential of this model to provide insight into the functional significance of similar activity in the basal ganglia in advanced PD. Increases in oscillatory activity in the basal ganglia are of special interest in PD as this activity is modulated during movement and reduced in conjunction with improvement in motor symptoms following L-dopa treatment (Brown and Williams, 2005;Jenkinson and Brown, 2011;Kuhn et al., 2006;Weinberger et al., 2006). The results show that LFPs and spiking activity in basal ganglia output in the dopamine deprived hemisphere of the hemiparkinsonian rat are dramatically different from those in the intact hemisphere under a range of behavioral states. Notably, in the dopamine cell-lesioned hemisphere, recordings show striking increases in synchronized spiking and oscillatory LFP activity in the high beta/low gamma range during alert non-walking, treadmill walking, grooming and REM sleep. The data also show that the expression of this oscillatory activity is affected by movement and L-dopa administration in ways consistent with responses of beta range oscillations in the STN and GPi in PD patients (Brittain and Brown, 2014;Brown and Williams, 2005;Jenkinson and Brown, 2011). These results support the utility of this rat model for exploration of mechanisms contributing to the exaggerated oscillatory activity in PD and its pathological relevance.

In particular, the present results show that the power of the exaggerated oscillatory activity in the SNpr of the hemiparkinsonian rat is modulated in conjunction with treadmill walking. Modulation of beta range activity in association with movement has been extensively explored in the basal ganglia of PD patients and its significance remains a subject of ongoing interest (Cassidy et al., 2002;Doyle et al., 2005;Florin et al., 2013;Foffani et al., 2005a;Hirschmann et al., 2013;Jenkinson and Brown, 2011;Joundi et al., 2013;Kempf et al., 2007;Kuhn et al., 2004;Priori et al., 2002;Wingeier et al., 2006). The exaggerated high beta/low gamma activity in the SNpr of the hemiparkinsonian rats appears most prominent during periods when the rats are executing repetitive movements, such as walking or grooming. When the rats are walking steadily on the circular treadmill, bursts of high beta/low gamma activity are evident in wavelet-based LFP scalograms from the SNpr of the lesioned hemisphere in correlation with the rat’s stepping cycle. The significant correlation between cycles of synchronization and desynchronization of SNpr 30–35 Hz activity and contralateral EMG activity shows that the amplitude of the exaggerated oscillatory activity is modulated in conjunction with the repetitive movements of the forelimb during walking.

SNpr LFP power in the 30–35 Hz frequency range was also consistently greater at the beginning of each walking epoch and declined over the first minutes of walking, leveling off at ~50% of peak power by 6 min. The decline in LFP power correlated with a reduction in the RMS of the EMG voltage. This attenuation in power and EMG variability as the rat gets

under way on the treadmill is intriguing in light of the greater difficulty PD patients have with initiation of walking, as opposed to maintenance once walking is in progress (Delval et al., 2014). It is also consistent with reports of 50% reduction in beta range activity observed in recordings from patients during (ongoing) voluntary movement (Jenkinson and Brown, 2011). In addition, exaggerated LFP activity was similarly evident, albeit at a slightly but significantly lower frequency (~28 Hz) than during regular walking, when the rats were in a non-walking but alert state, prompted by sounds such as crunching of paper or shaking of a rattle. Rats were not actively moving their limbs or head during these epochs (except for occasional movement of the whiskers). One could argue that this state may be similar to that of a patient sitting quietly but alert. A shift to increased power in lower frequencies with transition from treadmill walking to rest has also been noted in ECoG recordings from the hemiparkinsonian rat (Lehmkuhle et al., 2009).

Interestingly, exaggerated high beta/low gamma range activity was also observed in the dopamine-deprived hemisphere of the hemiparkinsonian rat during epochs of REM sleep. These epochs were marked by a twitching of the animal's limbs and whiskers, as is characteristic of the REM state. Although only two epochs of REM sleep were captured during the recordings made for this study, this activity provides another point of comparison with PD patients, as exaggerated oscillatory activity has also been recorded during REM sleep in the STN in these patients in the high beta (20–30 Hz) range (Urrestarazu et al., 2009). In the rat, dominant frequencies during the REM epochs were within a similar range, overlapping with the frequencies observed during alert non-walking epochs. Although preliminary, these data suggest that the mechanisms generating high beta range oscillations in the alert rat are also active during REM sleep.

In contrast to the epochs associated with REM, repetitive movement, or alert states, periods of inattentive rest were characterized by an increase in activity in a broad band over lower frequencies (<20 Hz) and a markedly reduced level of LFP oscillatory activity in the 25–40 Hz range in the lesioned hemisphere. Whether a comparable decrease in beta range activity is correlated with transition from alert states to inattentive rest in the PD patients is not clear. However, Urrestarazu and coauthors (Urrestarazu et al., 2009) report reduced levels of beta activity in PD patients during light (Stage 2) sleep, relative to awake states. Other investigators have commented on differences in how low vs. high beta range LFP power responds to activity and l-dopa in PD patients (Brittain and Brown, 2014;Foffani et al., 2005b;Litvak et al., 2011). These observations together with the somewhat bimodal distribution of spectral peaks in the low and high beta ranges seen collectively across studies (Chen et al., 2010; de Solages et al., 2010; Kuhn et al., 2009) leaves open the possibility that differencies in the relative spectral power within these 2 ranges may be linked to differences in arousal or attention in PD patients, as shown in the rodent model.

The design of the present study also allowed us to compare the dominant frequencies of the spike-LFP synchronization during awake states with dominent frequencies during urethane anesthesia with sensory stimulation in the same set of rats. Increases in beta range oscillatory LFP activity are observed in the basal ganglia in urethane anesthetized rats during global activation with sensory stimulation (Mallet et al., 2008a;Mallet et al., 2008b;Moran et al., 2011;Nevado-Holgado et al., 2014;Sharott et al., 2005). Notably, the

current results show that the dominant frequencies observed during this state (range 19–25 Hz, mean 21 Hz) are significantly different from those observed in the same rats while awake, regardless of state. These frequencies are also different from those observed during REM sleep.

As in the PD patient (Kuhn et al., 2006;Ray et al., 2008;Weinberger et al., 2006), the current results also show that L-dopa administration reduces exaggerated oscillatory activity in the SNpr in close correlation with a reduction in motor deficits in the hemiparkinsonian rat. The rats' ability to walk on the treadmill's narrow circular track when oriented in the direction contraversive to the lesion was improved by L-dopa administration in conjunction with a decrease in SNpr LFP power in the 25–40 Hz range, providing evidence for a link between loss of dopamine, SNpr LFP oscillatory activity, and walking deficits. Further indication of a significant correlation between these phenomena was obtained by two treatments believed to reduce the ability of L-dopa to compensate for the loss of dopamine. The serotonergic 1A agonist, 8-OH-DPAT, which reduces firing rates of serotonergic neurons (Aghajanian et al., 1990;Martin et al., 1999;Waterhouse et al., 2004), and the D2 dopamine receptor antagonist, eticlopride, blocked the effects of L-dopa on stepping ratios during contraversive walking. The effects of the 5HT1A agonist were reversed by administration of a 5HT1A antagonist. These results are consistent with the hypothesis that serotonergic neurons play a role in converting L-dopa to dopamine after dopamine cell death and facilitate the release of dopamine at sites innervated by serotonergic neurons (Carta et al., 2007;Carta et al., 2008b;Kannari et al., 2001;Maeda et al., 2005;Navailles et al., 2010). These effects are also consistent with evidence that serotonergic agonists can reduce dyskinetic behaviors in the rat model of L-dopa-induced dyskinesia (Carta et al., 2008a;Munoz et al., 2008;Tronci and Carta, 2013).

Collectively, the similarities between the modulatory effects of L-dopa and repetitive movement on exaggerated LFP activity in the hemiparkinsonian rats and in advanced PD patients argue that mechanisms underlying these dynamic changes in the rodent model are relevant to processes driving increased oscillatory activity in advanced cases of human PD. A number of mechanisms have been proposed to account for how loss of dopamine could promote increased synchronization of activity in the basal ganglia (McCarthy et al., 2011;Rubin et al., 2012;Stein and Bar-Gad, 2013;Weinberger and Dostrovsky, 2011). Alterations in cortical activity (Goldberg et al., 2002;Kerr et al., 2013;Li et al., 2007), enhanced response to cortical input at the level of the striatum (Kita and Kita, 2011b;Zold et al., 2012), or the STN (Marreiros et al., 2012;Wilson and Bevan, 2011;Yamawaki et al., 2012), modifications in STN-GPe network activity (Fan et al., 2012;Mallet et al., 2008a;Nevado-Holgado et al., 2014;Pavlides et al., 2012;Tachibana et al., 2011) as well as resonance activity emerging throughout the basal ganglia thalamocortical circuit may all contribute (Eusebio et al., 2009;Leblois et al., 2006; Montgomery, Jr., 2009; Moran et al., 2011; Van Albada et al., 2009; Wichmann and Smith, 2013). Evidence from the current study for different frequency ranges emerging during different activity states supports the idea that a range of processes and circuits contribute to the abnormally augmented activity which emerges in the basal ganglia output nuclei after loss of dopamine. The rodent data also indicate that plasticity continues to evolve within the affected networks over time. Over a period of 6–8 weeks post-lesion, the mean entrainment frequency of the spike activity

during treadmill walking increased slowly, but steadily, in the hemiparkinsonian rat, from 31 to 37 Hz, at a rate of about 1 Hz per week.

The differences in frequency ranges between behavioral states, across species, and over time are also relevant to whether abnormal oscillatory activity in a particular frequency range is responsible for the motor symptoms that accompany loss of dopamine. It has been suggested that the increase in 13–30 Hz beta range activity in human PD leads to motor symptoms by 'locking in' the state normally associated with this frequency range, one with reduced likelihood of voluntary activity (Jenkinson and Brown, 2011). As beta activity in the ~20 Hz range in the basal ganglia of the normal rat has been linked to a similar stabilized state (Leventhal et al., 2012), evidence for exaggerated activity at higher frequencies in the bradykinetic rats (30–35 Hz) and lower frequencies in bradykinetic primates (3–14 Hz) (Gatev et al., 2006;Heimer et al., 2006;Leblois et al., 2007;Raz et al., 2000;Tachibana et al., 2011) argues against a specific frequency range encouraging the emergence of bradykinesia across species.

While considering the inplications of these data, it is important to keep in mind the limitations of hemiparkinsonian rat as a model for PD. While this rodent model involves a rapid loss of dopamine neurons in one hemisphere, PD is associated with a more gradual loss of dopamine neurons, as well as other monoaminergic neurons, in both hemispheres. With respect to the unilateral loss of dopamine, preliminary studies (unpublished results) indicate that changes in SNpr LFP activity in rats with bilateral 6-OHDA lesions resemble those in the unilaterally lesioned rats. Thus, the unilateral nature of the model does not seem to be a confound with respect to the expression of beta/low gamma range oscillatory activity over the first 4–6 weeks post lesion. On the other hand, the rapidity of dopamine cell loss in this model makes it challenging to address the relative timing of the appearences of motor deficits and increases in oscillatory activity. Nevertheless, several studies have provided evidence of discrepancies in the time courses of these phenomena in the hemiparkinsonian rat (Degos et al., 2009;Dejean et al., 2012;Ellens and Leventhal, 2013;Mallet et al., 2008b;Quiroga-Varela et al., 2013).

In summary, the present study characterizes frequency-specific increases in oscillatory activity in basal ganglia output of the hemiparkinsonian rat over a series of behaviors. The dominant frequencies of spike-LFP entrainment are dependent on behavioral state. SNpr LFP amplitude and spike-LFP entrainment in the lesioned hemisphere of the rodent model is modulated by motor activity over a range of time scales. Reduction of LFP power and spike-LFP entrainment by L-dopa administration is correlated with attenuation of motor deficits and reversed by serotoninergic 1a receptor stimulation. Results highlight the similaries and differences between exaggerated oscillatory activity in the hemiparkinsonian rat and human PD and the utility of this model for exploring mechanisms promoting these increases in synchronized activity and their role in induction of motor symptoms in PD.

Acknowledgements

The Intramural Research Program of the NINDS, NIH supported this research. We wish to thank Newlin, Morgan, Tom Talbot and Daryl Brandy in the Research Services Branch for design and fabrication of the rotary treadmill.

REFERENCES

Aghajanian GK, Sprouse JS, Sheldon P, Rasmussen K. Electrophysiology of the central serotonin system: receptor subtypes and transducer mechanisms. Ann N Y Acad Sci. 1990; 600:93–103. [PubMed: 2123618]

Alonso-Frech F, Zamarbide I, Alegre M, Rodriguez-Oroz MC, Guridi J, Manrique M, Valencia M, Artieda J, Obeso JA. Slow oscillatory activity and levodopa-induced dyskinesias in Parkinson's disease. Brain. 2006; 129:1748–1757. [PubMed: 16684788]

Avila I, Parr-Brownlie LC, Brazhnik E, Castaneda E, Bergstrom DA, Walters JR. Beta frequency synchronization in basal ganglia output during rest and walk in a hemiparkinsonian rat. Exp Neurol. 2010; 221:307–319. [PubMed: 19948166]

Belluscio MA, Escande MV, Keifman E, Riquelme LA, Murer MG, Zold CL. Oscillations in the basal ganglia in Parkinson's disease: Role of the striatum. Basal Ganglia. 2013 in press.

Bergman H, Wichmann T, Karmon B, Delong MR. The primate subthalamic nucleus. II. Neuronal activity in the MPTP model of parkinsonism. J Neurophys. 1994; 72:507–520.

Brazhnik E, Cruz AV, Avila I, Wahba MI, Novikov N, Ilieva NM, McCoy AJ, Gerber C, Walters JR. State-Dependent Spike and Local Field Synchronization between Motor Cortex and Substantia Nigra in Hemiparkinsonian Rats. J Neurosci. 2012; 32:7869–7880. [PubMed: 22674263]

Brittain JS, Brown P. Oscillations and the basal ganglia: motor control and beyond. Neuroimage. 2014; 85(Pt 2):637–647. [PubMed: 23711535]

Brown P. Oscillatory nature of human basal ganglia activity: Relationship to the pathophysiology of Parkinson's disease. Mov Disord. 2003; 18:357–363. [PubMed: 12671940]

Brown P, Oliviero A, Mazzone P, Insola A, Tonali P, Di Lazzaro V. Dopamine dependency of oscillations between subthalamic nucleus and pallidum in Parkinson's disease. J Neurosci. 2001; 21:1033–1038. [PubMed: 11157088]

Brown P, Williams D. Basal ganglia local field potential activity: character and functional significance in the human. Clin Neurophysiol. 2005; 116:2510–2519. [PubMed: 16029963]

Carta M, Carlsson T, Kirik D, Bjorklund A. Dopamine released from 5-HT terminals is the cause of L-DOPA-induced dyskinesia in parkinsonian rats. Brain. 2007; 130:1819–1833. [PubMed: 17452372]

Carta M, Carlsson T, Munoz A, Kirik D, Bjorklund A. Involvement of the serotonin system in L-dopa-induced dyskinesias. Parkinsonism Relat Disord. 2008a; 14(Suppl 2):S154–S158. [PubMed: 18579429]

Carta M, Carlsson T, Munoz A, Kirik D, Bjorklund A. Serotonin-dopamine interaction in the induction and maintenance of L-DOPA-induced dyskinesias. Prog Brain Res. 2008b; 172:465–478. [PubMed: 18772046]

Cassidy M, Mazzone P, Oliviero A, Insola A, Tonali P, Di Lazzaro V, Brown P. Movement-related changes in synchronization in the human basal ganglia. Brain. 2002; 125:1235–1246. [PubMed: 12023312]

Chen CC, Hsu YT, Chan HL, Chiou SM, Tu PH, Lee ST, Tsai CH, Lu CS, Brown P. Complexity of subthalamic 13–35 Hz oscillatory activity directly correlates with clinical impairment in patients with Parkinson's disease. Exp Neurol. 2010; 224:234–240. [PubMed: 20353774]

de Solages C, Hill BC, Koop MM, Henderson JM, Bronte-Stewart H. Bilateral symmetry and coherence of subthalamic nuclei beta band activity in Parkinson's disease. Exp Neurol. 2010; 221:260–266. [PubMed: 19944098]

Degos B, Deniau J-M, Chavez M, Maurice N. Chronic but not acute dopaminergic transmission interruption promotes a progressive increase in cortical beta frequency synchronization: relationships to vigilance state and akinesia. Cereb Cortex. 2009:1616–1630. [PubMed: 18996909]

Dejean C, Nadjar A, Le MC, Bioulac B, Gross CE, Boraud T. Evolution of the dynamic properties of the cortex-basal ganglia network after dopaminergic depletion in rats. Neurobiol Dis. 2012; 46:402–413. [PubMed: 22353564]

Delaville C, Cruz AV, McCoy AJ, Brazhnik E, Avila I, Novikov N, Walters JR. Oscillatory activity in basal ganglia and motor cortex in an awake behaving rodent model of Parkinson's disease. Basal Ganglia. 2014; 3:221–227.

Delval A, Tard C, Defebvre L. Why we should study gait initiation in Parkinson's disease. Neurophysiol Clin. 2014; 44:69–76. [PubMed: 24502907]

Doyle LMF, Kuhn AA, Hariz M. Levodopa-induced modulation of subthalamic beta oscillations during self-paced movements in patients with Parkinson's disease. Eur J Neurosci. 2005; 21:1403–1412. [PubMed: 15813950]

Ellens DJ, Leventhal DK. Review: electrophysiology of basal ganglia and cortex in models of Parkinson disease. J Parkinsons Dis. 2013; 3:241–254. [PubMed: 23948994]

Eusebio A, Pogosyan A, Wang S, Averbeck B, Gaynor LD, Cantiniaux S, Witjas T, Limousin P, Azulay JP, Brown P. Resonance in subthalamo-cortical circuits in Parkinson's disease. Brain. 2009; 132:2139–2150. [PubMed: 19369488]

Fan KY, Baufreton J, Surmeier DJ, Chan CS, Bevan MD. Proliferation of external globus pallidus-subthalamic nucleus synapses following degeneration of midbrain dopamine neurons. J Neurosci. 2012; 32:13718–13728. [PubMed: 23035084]

Florin E, Dafsari HS, Reck C, Barbe MT, Pauls KA, Maarouf M, Sturm V, Fink GR, Timmermann L. Modulation of local field potential power of the subthalamic nucleus during isometric force generation in patients with Parkinson's disease. Neuroscience. 2013; 240:106–116. [PubMed: 23454540]

Foffani G, Bianchi AM, Baselli G, Priori A. Movement-related frequency modulation of beta oscillatory activity in the human subthalamic nucleus. J Physiol. 2005a; 568:699–711. [PubMed: 16123109]

Foffani G, Priori A, Ardolino, Bossi, Carrabba, Egidi, Locatelli, Caputo M, Tamma, Baselli, Bianchi A, Cerutti S. Multiple independent subthalamic rhythms in patients with Parkinson's disease. Mov Disord. 2005b; 20:S86.

Fries P, Reynolds JH, Rorie AE, Desimone R. Modulation of oscillatory neuronal synchronization by selective visual attention. Science. 2001; 291:1560–1563. [PubMed: 11222864]

Gatev P, Darbin O, Wichmann T. Oscillations in the basal ganglia under normal conditions and in movement disorders. Mov Disord. 2006; 21:1566–1577. [PubMed: 16830313]

Goldberg JA, Boraud T, Maraton S, Haber SN, Vaadia E, Bergman H. Enhanced synchrony among primary motor cortex neurons in the 1-methyl-4-phenyl-1,2,3,6-tetrahydropyridine primate model of Parkinson's disease. J Neurosci. 2002; 22:4639–4653. [PubMed: 12040070]

Heimer G, Rivlin-Etzion M, Bar-Gad I, Goldberg JA, Haber SN, Bergman H. Dopamine replacement therapy does not restore the full spectrum of normal pallidal activity in the 1-methyl-4-phenyl-1,2,3,6-tetra-hydropyridine primate model of Parkinsonism. J Neurosci. 2006; 26:8101–8114. [PubMed: 16885224]

Hirschmann J, Ozkurt TE, Butz M, Homburger M, Elben S, Hartmann CJ, Vesper J, Wojtecki L, Schnitzler A. Differential modulation of STN-cortical and cortico-muscular coherence by movement and levodopa in Parkinson's disease. Neuroimage. 2013; 68:203–213. [PubMed: 23247184]

Jenkinson N, Brown P. New insights into the relationship between dopamine, beta oscillations and motor function. Trends Neurosci. 2011; 34:611–618. [PubMed: 22018805]

Joundi RA, Brittain JS, Green AL, Aziz TZ, Brown P, Jenkinson N. Persistent suppression of subthalamic beta-band activity during rhythmic finger tapping in Parkinson's disease. Clin Neurophysiol. 2013; 124:565–573. [PubMed: 23085388]

Kannari K, Yamato H, Shen H, Tomiyama M, Suda T, Matsunaga M. Activation of 5-HT(1A) but not 5-HT(1B) receptors attenuates an increase in extracellular dopamine derived from exogenously administered L-DOPA in the striatum with nigrostriatal denervation. J Neurochem. 2001; 76:1346–1353. [PubMed: 11238719]

Kempf F, Kuhn AA, Kupsch A, Brucke C, Weise L, Schneider GH, Brown P. Premovement activities in the subthalamic area of patients with Parkinson's disease and their dependence on task. Eur J Neurosci. 2007; 25:3137–3145. [PubMed: 17561827]

Kerr CC, Van Albada SJ, Neymotin SA, Chadderdon GL, Robinson PA, Lytton WW. Cortical information flow in Parkinson's disease: a composite network/field model. Front Comput Neurosci. 2013; 7:39. [PubMed: 23630492]

Kita H, Kita T. Cortical stimulation evokes abnormal responses in the dopamine-depleted rat basal ganglia. J Neurosci. 2011a; 31:10311–10322. [PubMed: 21753008]

Kita H, Kita T. Role of Striatum in the Pause and Burst Generation in the Globus Pallidus of 6-OHDA-Treated Rats. Front Syst Neurosci. 2011b; 5:42. [PubMed: 21713126]

Kuhn AA, Kupsch A, Schneider GH, Brown P. Reduction in subthalamic 8–35 Hz oscillatory activity correlates with clinical improvement in Parkinson's disease. Eur J Neurosci. 2006; 23:1956–1960. [PubMed: 16623853]

Kuhn AA, Trottenberg T, Kivi A, Kupsch A, Schneider GH, Brown P. The relationship between local field potential and neuronal discharge in the subthalamic nucleus of patients with Parkinson's disease. Exp Neurol. 2005; 194:212–220. [PubMed: 15899258]

Kuhn AA, Tsui A, Aziz T, Ray N, Brucke C, Kupsch A, Schneider GH, Brown P. Pathological synchronisation in the subthalamic nucleus of patients with Parkinson's disease relates to both bradykinesia and rigidity. Exp Neurol. 2009; 215:380–387. [PubMed: 19070616]

Kuhn AA, Williams D, Kupsch A, Limousin P, Hariz M, Schneider GH, Yarrow K, Brown P. Event-related beta desynchronization in human subthalamic nucleus correlates with motor performance. Brain. 2004; 127:735–746. [PubMed: 14960502]

Leblois A, Boraud T, Meissner W, Bergman H, Hansel D. Competition between feedback loops underlies normal and pathological dynamics in the basal ganglia. J Neurosci. 2006; 26:3567–3583. [PubMed: 16571765]

Leblois A, Meissner W, Bioulac B, Gross CE, Hansel D, Boraud T. Late emergence of synchronized oscillatory activity in the pallidum during progressive Parkinsonism. Eur J Neurosci. 2007; 26:1701–1713. [PubMed: 17880401]

Lehmkuhle MJ, Bhangoo SS, Kipke DR. The Electrocorticogram Signal Can Be Modulated With Deep Brain Stimulation of the Subthalamic Nucleus in the Hemiparkinsonian Rat. Journal of Neurophysiology. 2009; 102:1811–1820. [PubMed: 19625533]

Leventhal DK, Gage GJ, Schmidt R, Pettibone JR, Case AC, Berke JD. Basal ganglia beta oscillations accompany cue utilization. Neuron. 2012; 73:523–536. [PubMed: 22325204]

Levy R, Hutchison WD, Lozano AM, Dostrovsky JO. Synchronized neuronal discharge in the basal ganglia of parkinsonian patients is limited to oscillatory activity. J Neurosci. 2002; 22:2855–2861. [PubMed: 11923450]

Li S, Arbuthnott GW, Jutras MJ, Goldberg JA, Jaeger D. Resonant antidromic cortical circuit activation as a consequence of high-frequency subthalamic deep-brain stimulation. J Neurophysiol. 2007; 98:3525–3537. [PubMed: 17928554]

Lindgren HS, Andersson DR, Lagerkvist S, Nissbrandt H, Cenci MA. L-DOPA-induced dopamine efflux in the striatum and the substantia nigra in a rat model of Parkinson's disease: temporal and quantitative relationship to the expression of dyskinesia. J Neurochem. 2010; 112:1465–1476. [PubMed: 20050978]

Litvak V, Jha A, Eusebio A, Oostenveld R, Foltynie T, Limousin P, Zrinzo L, Hariz MI, Friston K, Brown P. Resting oscillatory cortico-subthalamic connectivity in patients with Parkinson's disease. Brain. 2011; 134:359–374. [PubMed: 21147836]

Maeda T, Nagata K, Yoshida Y, Kannari K. Serotonergic hyperinnervation into the dopaminergic denervated striatum compensates for dopamine conversion from exogenously administered l-DOPA. Brain Res. 2005; 1046:230–233. [PubMed: 15894297]

Mallet N, Pogosyan A, Marton LF, Bolam JP, Brown P, Magill PJ. Parkinsonian Beta Oscillations in the External Globus Pallidus and Their Relationship with Subthalamic Nucleus Activity. J Neurosci. 2008a; 28:14245–14258. [PubMed: 19109506]

Mallet N, Pogosyan A, Sharott A, Csicsvari J, Bolam JP, Brown P, Magill PJ. Disrupted dopamine transmission and the emergence of exaggerated beta oscillations in subthalamic nucleus and cerebral cortex. J Neurosci. 2008b; 28:4795–4806. [PubMed: 18448656]

Marreiros AC, Cagnan H, Moran RJ, Friston KJ, Brown P. Basal ganglia-cortical interactions in Parkinsonian patients. Neuroimage. 2012; 66C:301–310. [PubMed: 23153964]

Martin LP, Jackson DM, Wallsten C, Waszczak BL. Electrophysiological comparison of 5-Hydroxytryptamine 1A receptor antagonists on dorsal raphe cell firing. J Pharmacol Exp Ther. 1999; 288:820–826. [PubMed: 9918594]

McCarthy MM, Moore-Kochlacs C, Gu X, Boyden ES, Han X, Kopell N. Striatal origin of the pathologic beta oscillations in Parkinson's disease. Proc Natl Acad Sci U S A. 2011; 108:11620–11625. [PubMed: 21697509]

Montgomery EB Jr. Basal ganglia pathophysiology in Parkinson's disease. Ann Neurol. 2009; 65:618. [PubMed: 19475660]

Moran RJ, Mallet N, Litvak V, Dolan RJ, Magill PJ, Friston KJ, Brown P. Alterations in Brain Connectivity Underlying Beta Oscillations in Parkinsonism. PLoS Comput Biol. 2011; 7

Munoz A, Li Q, Gardoni F, Marcello E, Qin C, Carlsson T, Kirik D, Di LM, Bjorklund A, Bezard E, Carta M. Combined 5-HT1A and 5-HT1B receptor agonists for the treatment of L-DOPA-induced dyskinesia. Brain. 2008; 131:3380–3394. [PubMed: 18952677]

Murer MG, Tseng KY, Kasanetz F, Belluscio M, Riquelme LA. Brain oscillations, medium spiny neurons, and dopamine. Cell Mol Neurobiol. 2002; 22:611–632. [PubMed: 12585682]

Navailles S, Bioulac B, Gross C, De DP. Serotonergic neurons mediate ectopic release of dopamine induced by L-DOPA in a rat model of Parkinson's disease. Neurobiol Dis. 2010; 38:136–143. [PubMed: 20096781]

Nevado-Holgado AJ, Mallet N, Magill PJ, Bogacz R. Effective connectivity of the subthalamic nucleus-globus pallidus network during Parkinsonian oscillations. J Physiol. 2014; 592:1429–1455. [PubMed: 24344162]

Olsson M, Nikkhah G, Bentlage C, Bjorklund A. Forelimb akinesia in the rat Parkinson model: differential effects of dopamine agonists and nigral transplants as assessed by a new stepping test. J Neurosci. 1995; 15:3863–3875. [PubMed: 7751951]

Pavlides A, Hogan SJ, Bogacz R. Improved conditions for the generation of beta oscillations in the subthalamic nucleus--globus pallidus network. Eur J Neurosci. 2012; 36:2229–2239. [PubMed: 22805067]

Politis M, Wu K, Loane C, Brooks DJ, Kiferle L, Turkheimer FE, Bain P, Molloy S, Piccini P. Serotonergic mechanisms responsible for levodopa-induced dyskinesias in Parkinson's disease patients. J Clin Invest. 2014; 124:1340–1349. [PubMed: 24531549]

Priori A, Foffani G, Pesenti A, Bianchi A, Chiesa V, Baselli G, Caputo E, Tamma F, Rampini P, Egidi M, Locatelli M, Barbieri S, Scarlato G. Movement-related modulation of neural activity in human basal ganglia and its L-DOPA dependency: recordings from deep brain stimulation electrodes in patients with Parkinson's disease. Neurological Sciences. 2002; 23:S101–S102. [PubMed: 12548363]

Priori A, Foffani G, Pesenti A, Tamma F, Bianchi AM, Pellegrini M, Locatelli M, Moxon KA, Villani RM. Rhythm-specific pharmacological modulation of subthalamic activity in Parkinson's disease. Exp Neurol. 2004; 189:369–379. [PubMed: 15380487]

Quiroga-Varela A, Walters JR, Brazhnik E, Marin C, Obeso JA. What basal ganglia changes underlie the parkinsonian state? The significance of neuronal oscillatory activity. Neurobiol Dis. 2013; 58:242–248. [PubMed: 23727447]

Ray NJ, Jenkinson N, Wang S, Holland P, Brittain JS, Joint C, Stein JF, Aziz T. Local field potential beta activity in the subthalamic nucleus of patients with Parkinson's disease is associated with improvements in bradykinesia after dopamine and deep brain stimulation. Exp Neurol. 2008; 213:108–113. [PubMed: 18619592]

Raz A, Frechter-Mazar V, Feingold A, Abeles M, Vaadia E, Bergman H. Activity of pallidal and striatal tonically active neurons is correlated in mptp-treated monkeys but not in normal monkeys. J Neurosci. 2001; 21:RC128. [PubMed: 11157099]

Raz A, Vaadia E, Bergman H. Firing patterns and correlations of spontaneous discharge of pallidal neurons in the normal and the tremulous 1-methyl-4-phenyl-1,2,3,6-tetrahydropyridine vervet model of parkinsonism. J Neurosci. 2000; 20:8559–8571. [PubMed: 11069964]

Rubin JE, McIntyre CC, Turner RS, Wichmann T. Basal ganglia activity patterns in parkinsonism and computational modeling of their downstream effects. Eur J Neurosci. 2012; 36:2213–2228. [PubMed: 22805066]

Schallert, T.; Tillerson, J. Intervention strategies for degeneration of dopamine neurons in parkinsonism: optimizing behavioral assessment of outcome. In: Emerich, D.; Dean, R.; Sanberg, P., editors. Central Nervous System Diseases. Totowa, NJ: Humana Press Inc; 1999. p. 131-151.

Sharott A, Magill PJ, Harnack D, Kupsch A, Meissner W, Brown P. Dopamine depletion increases the power and coherence of beta-oscillations in the cerebral cortex and subthalamic nucleus of the awake rat. Eur J Neurosci. 2005; 21:1413–1422. [PubMed: 15813951]

Stein E, Bar-Gad I. Beta oscillations in the cortico-basal ganglia loop during parkinsonism. Exp Neurol. 2013; 245:52–59. [PubMed: 22921537]

Tachibana Y, Iwamuro H, Kita H, Takada M, Nambu A. Subthalamo-pallidal interactions underlying parkinsonian neuronal oscillations in the primate basal ganglia. Eur J Neurosci. 2011; 34:1470–1484. [PubMed: 22034978]

Tronci E, Carta M. 5-HT1 receptor agonists for the treatment of L-DOPA-induced dyskinesia: From animal models to clinical investigation. Basal Ganglia. 2013; 3:9–13.

Tseng KY, Kasanetz F, Kargieman L, Riquelme LA, Murer MG. Cortical slow oscillatory activity is reflected in the membrane potential and spike trains of striatal neurons in rats with chronic nigrostriatal lesions. J Neurosci. 2001; 21:6430–6439. [PubMed: 11487667]

Urrestarazu E, Iriarte J, Alegre M, Clavero P, Rodriguez-Oroz MC, Guridi J, Obeso JA, Artieda J. Beta activity in the subthalamic nucleus during sleep in patients with Parkinson's disease. Mov Disord. 2009; 24:254–260. [PubMed: 18951542]

Van Albada SJ, Gray RT, Drysdale PM, Robinson PA. Mean-field modeling of the basal ganglia-thalamocortical system. II Dynamics of parkinsonian oscillations. J Theor Biol. 2009; 257:664–688. [PubMed: 19154745]

Walters JR, Hu D, Itoga CA, Parr-Brownlie LC, Bergstrom DA. Phase relationships support a role for coordinated activity in the indirect pathway in organizing slow oscillations in basal ganglia output after loss of dopamine. Neuroscience. 2007; 144:762–776. [PubMed: 17112675]

Waterhouse BD, Devilbiss D, Seiple S, Markowitz R. Sensorimotor-related discharge of simultaneously recorded, single neurons in the dorsal raphe nucleus of the awake, unrestrained rat. Brain Res. 2004; 1000:183–191. [PubMed: 15053966]

Weinberger M, Dostrovsky JO. A basis for the pathological oscillations in basal ganglia: the crucial role of dopamine. Neuroreport. 2011; 22:151–156. [PubMed: 21304324]

Weinberger M, Mahant N, Hutchison WD, Lozano AM, Moro E, Hodaie M, Lang AE, Dostrovsky JO. Beta oscillatory activity in the subthalamic nucleus and its relation to dopaminergic response in Parkinson's disease. J Neurophysiol. 2006; 96:3248–3256. [PubMed: 17005611]

Wichmann T, Smith Y. Extrastriatal plasticity in parkinsonism. Basal Ganglia. 2013; 3:5–8.

Wilson CJ, Bevan MD. Intrinsic dynamics and synaptic inputs control the activity patterns of subthalamic nucleus neurons in health and in Parkinson's disease. Neuroscience. 2011; 198:54–68. [PubMed: 21723918]

Wingeier B, Tcheng T, Koop MM, Hill BC, Heit G, Bronte-Stewart HM. Intra-operative STN DBS attenuates the prominent beta rhythm in the STN in Parkinson's disease. Exp Neurol. 2006; 197:244–251. [PubMed: 16289053]

Yamawaki N, Magill PJ, Woodhall GL, Hall SD, Stanford IM. Frequency selectivity and dopamine-dependence of plasticity at glutamatergic synapses in the subthalamic nucleus. Neuroscience. 2012; 203:1–11. [PubMed: 22209920]

Zold CL, Escande MV, Pomata PE, Riquelme LA, Murer MG. Striatal NMDA receptors gate corticopallidal synchronization in a rat model of Parkinson's disease. Neurobiol Dis. 2012; 47:38–48. [PubMed: 22465187]

Highlights

- Oscillatory activity in basal ganglia output is increased in the hemiparkinsonian rat
- Increases in LFP power are modulated by repetitive motor activity
- Spike-LFP entrainment frequencies vary with rest, alert, walking, and anesthesia
- L-dopa effect on LFP-spike entrainment is modulated by 5HT1a receptor stimulation

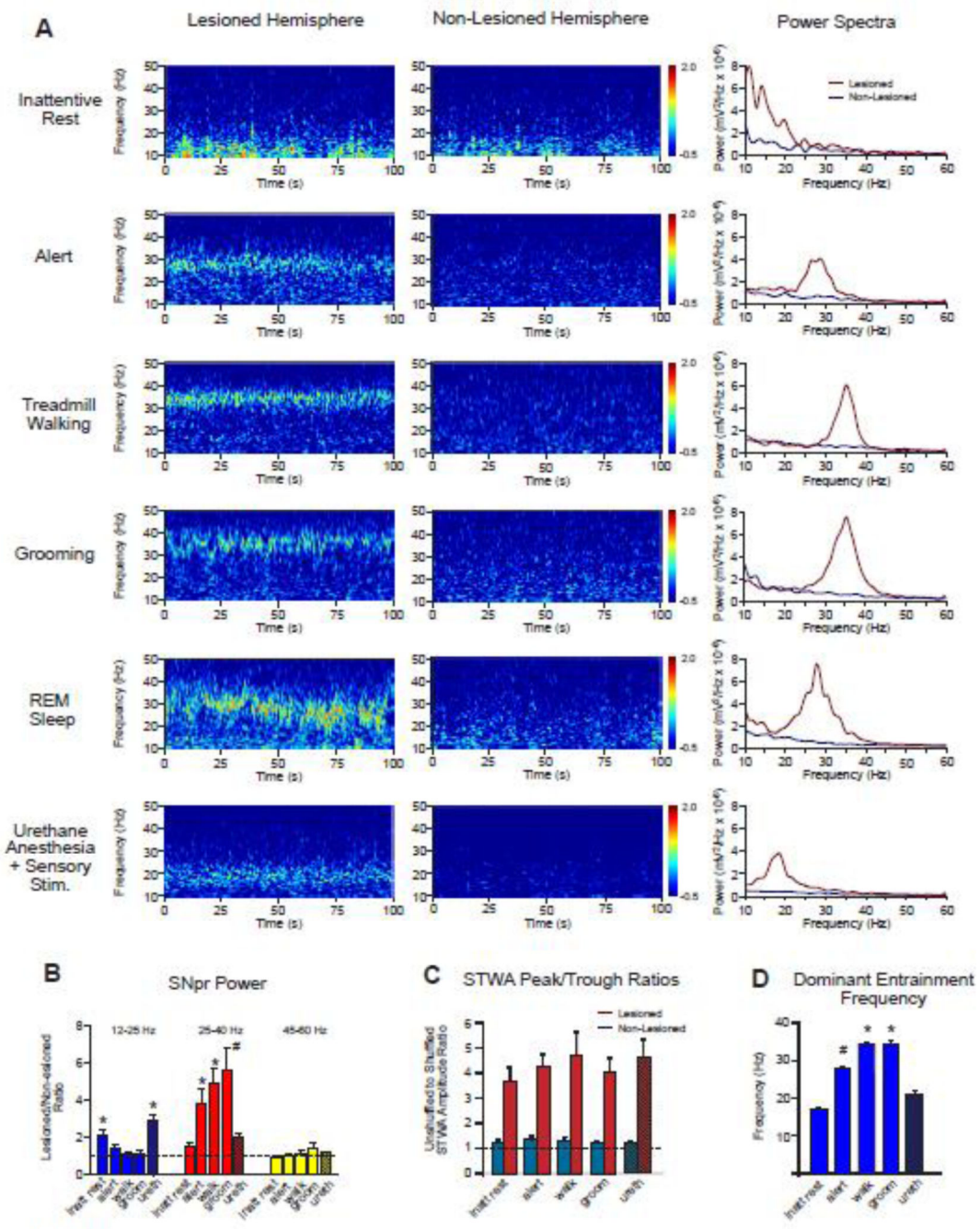

Figure 1.

SNpr LFP power, spike-LFP synchronization and dominant frequency in the dopamine cell-lesioned hemisphere, as compared to the non-lesioned hemisphere, during different behaviors and under urethane anesthesia. **A:** Wavelet-based scalograms of LFP spectral power in the SNpr from dopamine cell-lesioned and non-lesioned hemispheres (left and middle panels) show periods of inattentive rest, alert, ipsiversive treadmill walking, grooming, rapid eye movement (REM) sleep and during urethane anesthesia with sensory stimulation (urethane+SS). Spectral power is shown on a logarithmic scale with greater

power being represented by red colors. With the exception of the REM sleep and urethane epochs, examples are from the same rat on day 21 post-lesion. Episodes of REM sleep were recorded infrequently, and an example of one is shown here. Corresponding FFT-based LFP power spectra on the right represent the same epochs as shown in the scalograms. Note the marked increases in high beta/low gamma power in the lesioned hemisphere relative to the non-lesioned hemisphere during alert, treadmill walking and grooming, with increases in a lower beta range under urethane+SS. **B:** Bar graphs show mean ratios of SNpr LFP power in the dopamine cell-lesioned hemisphere relative to SNpr LFP power in the corresponding intact hemisphere for the ranges of 12–25 Hz (blue), 25–40 Hz (red) and 45–60 Hz (yellow) during inattentive rest (inatt rest), alert non-walking (alert), ipsiversive walking (walk), and grooming (groom) states (n=9), and under urethane+SS (ureth) (n=8). Data were averaged per rat. Dashed line represents a ratio of 1, indicating identical power in lesioned and non-lesioned hemispheres. In the 12–25 Hz range: * $p<0.02$ compared with alert, walk and grooming. In the 25–40 Hz range: * $p<0.003$ compared with rest and urethane. # $p<0.03$ compared with rest, alert and urethane+SS (1-way RM ANOVA. **C:** Spike-LFP synchronization in the 12–45 Hz range in the dopamine cell-lesioned hemisphere (red) and non-lesioned hemisphere (blue) over a range of behavioral states as reflected by the ratio of STWA-based peak-to-trough amplitudes of unshuffled vs. shuffled multiunit spike trains (4 spike trains over two epochs per behavior per rat, n=9 rats). Dashed line represents a ratio of 1, indicating that STWA peak-to-trough amplitudes from shuffled and unshuffled spike trains are equal. Note large differences in mean STWA peak-to-trough amplitude ratios in the dopamine lesioned hemisphere relative to the non-lesioned hemisphere showing greater phase-locking of spikes with LFP in the dopamine-depleted hemisphere (2-way RM ANOVA, $p<0.001$). See STWA waveform example for lesioned hemisphere in Fig 7. **A D:** Bar graph shows mean STWA-based dominant multiunit entrainment frequencies in SNpr LFP activity for spike trains that were significantly phase-locked to LFP (see Methods) in the low beta-low gamma range (12–45 Hz) in the dopamine cell-lesioned hemisphere during the same behavioral states as represented in A. * $p<0.05$ compared to rest, alert and urethane +SS,; # $p<0.05$ compared to rest and urethane+SS (1-way RM ANOVA). n= 31,30, 29, 28, and 29 for rest, alert, walk groom and urethane, respectively.

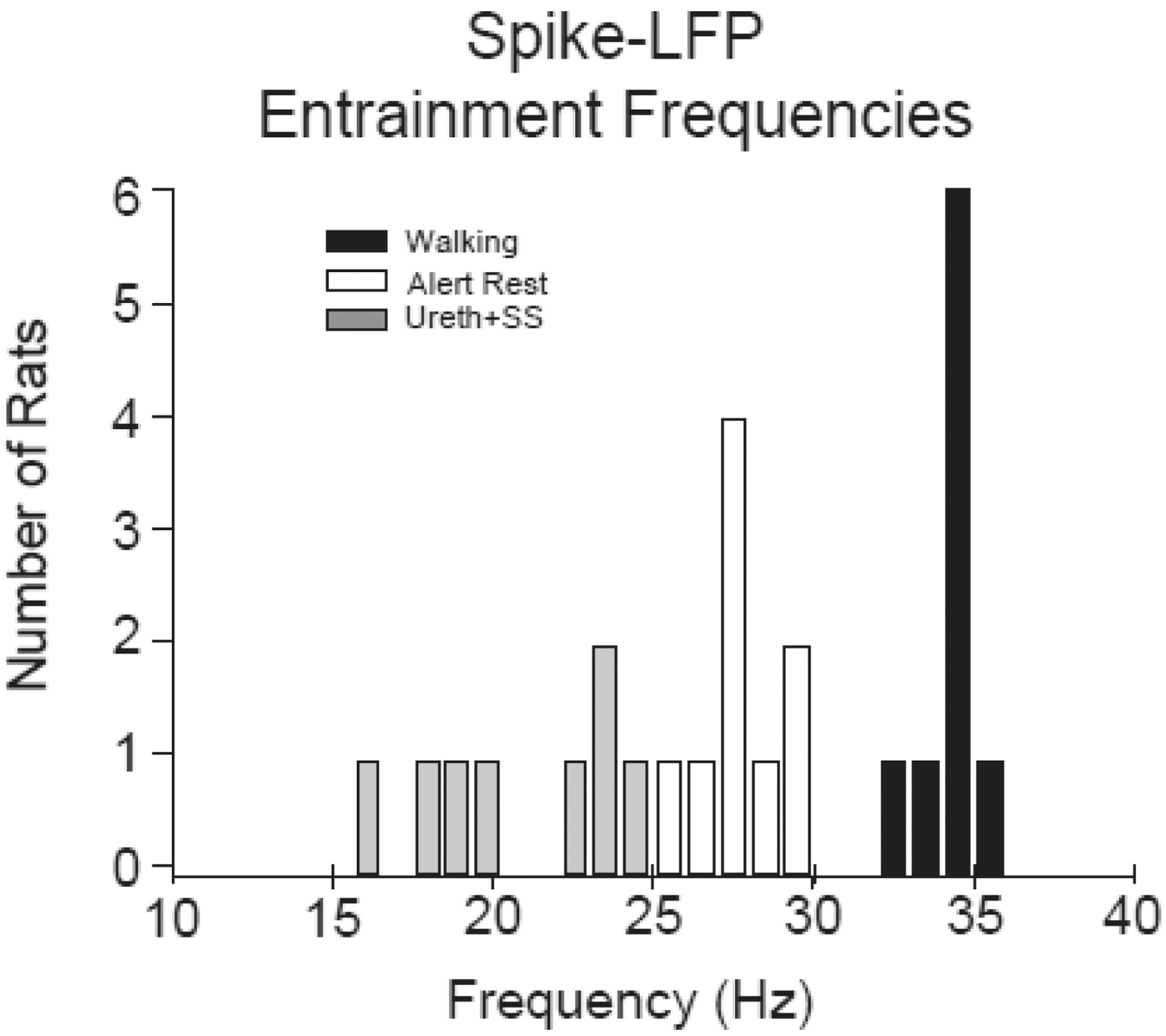

Figure 2.

The distribution of dominant frequencies in SNpr LFP activity in the 12–45 Hz range in the dopamine cell-lesioned hemisphere for epochs of alert rest, treadmill walking and under urethane anesthesia with sensory stimuli (ureth+SS). Data for alert and treadmill walking were from days 18–23 and from urethane+SS days 40–50. Dominant frequencies were obtained from SNpr multiunit spike trains significantly phase-locked to LFPs from 4 electrodes over four 30 s representative epochs as described in methods. Data were averaged per rat. Urethane: grey bars, n=8; walking: black bars, n=9; alert: white bars, n=9.

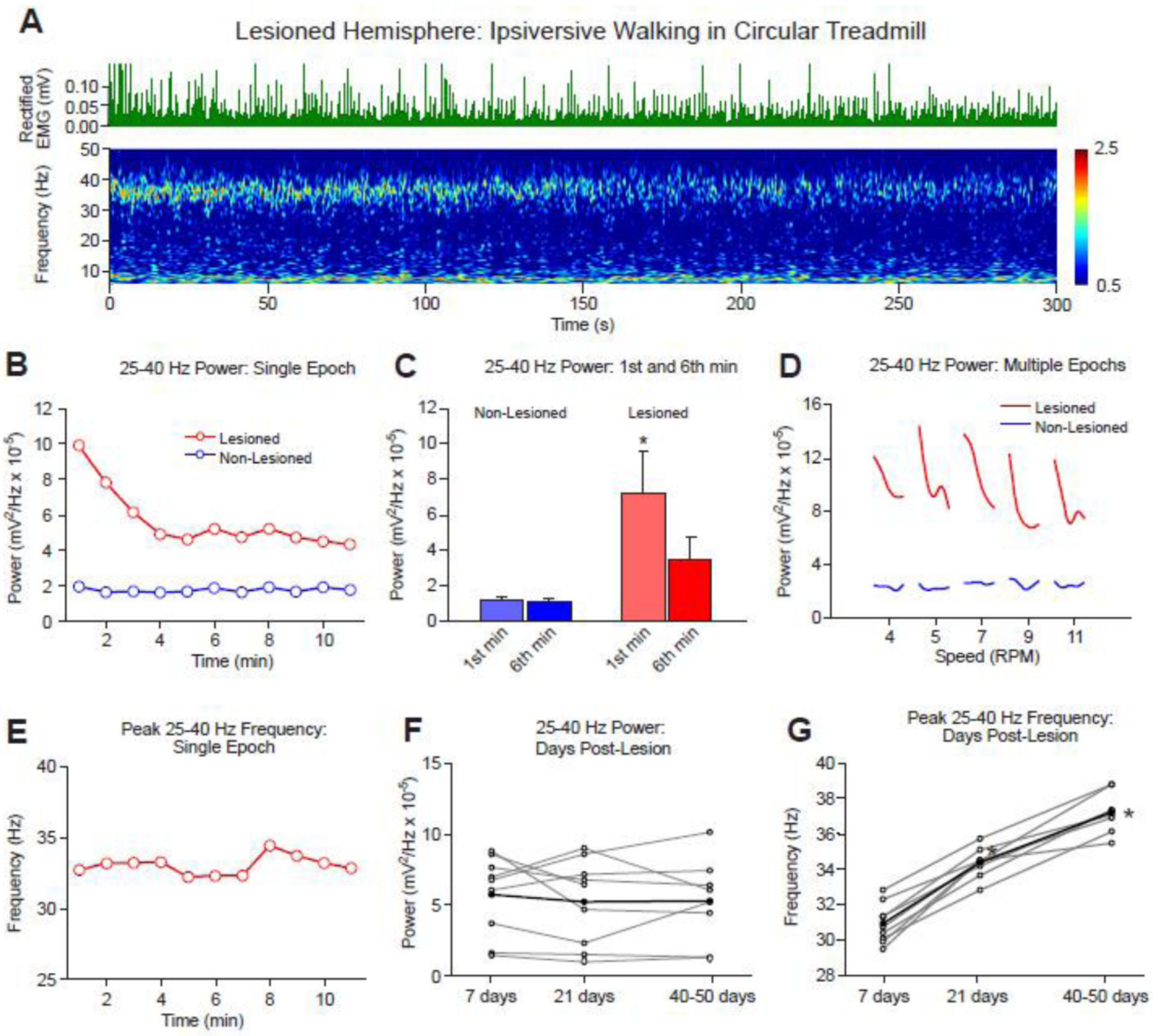

Figure 3.

Time-dependent changes in the 25–40 Hz range SNpr LFP power and dominant frequency in the dopamine cell-lesioned hemisphere relative to the non-lesioned hemisphere during ipsiversive treadmill walking. **A:** Wavelet-based scalogram shows a typical example of SNpr LFP power in the dopamine cell-lesioned hemisphere during the first 5 min of a walking epoch on day 43 post-lesion. Rectified EMG (green upper traces) recorded from the deltoid shoulder muscle shows consistent muscle activity during the walking epoch. Note that the high beta/low gamma range band shows reduction in power over time during the walking period. **B:** FFT-based SNpr LFP power in the 25–40 Hz range for consecutive 60s segments over an extended period of the same walking epoch as shown in A in the dopamine cell lesioned (red) and non-lesioned hemisphere (blue). Note a reduction in total power in the lesioned hemisphere over the first 4 min of walking. **C:** Bars show the 25–40

Hz LFP total power range for 1st and 6th min of walking for dopamine cell-lesioned vs non-lesioned hemispheres (n=9) at days 18–23 post lesion. * $p < 0.05$ compared to the non-lesioned hemisphere and 6th min within the lesioned hemisphere (2-way RM ANOVA). **D:** SNpr high beta/low gamma range (25–40 Hz) power in the lesioned hemisphere for 5 consecutive 2.5 min walking epochs (averaged over 30 s segments) over a range of treadmill speeds with 1 min rest epochs in between. Power was consistently reduced after the onset of walking, as in A and B. No change in power was observed in the non-lesioned hemisphere. A typical example is shown (N=6 rats). **E:** STWA-based entrainment frequency in SNpr LFP power spectra for consecutive 60 s segments of the walking epoch shown in A. Unlike power (in B), peak frequency in SNpr LFP spectral power remains stable over time of treadmill walking in the lesioned hemisphere. **F, G:** Line plots in F (gray lines) show the total LFP power in the 25–40 Hz range for individual rats from post-lesion day 7 up to 50 days. Mean power (black line) remains stable over days (n=9). In contrast, as shown in G, the dominant frequency during walking is significantly increased over the same time period between days 7 (31.0±0.9 Hz), 21 (34.0±0.3 Hz) and 40 post-lesion (36.7±0.4 Hz) (1-way RM ANOVA, * $p<0.001$, n=9).

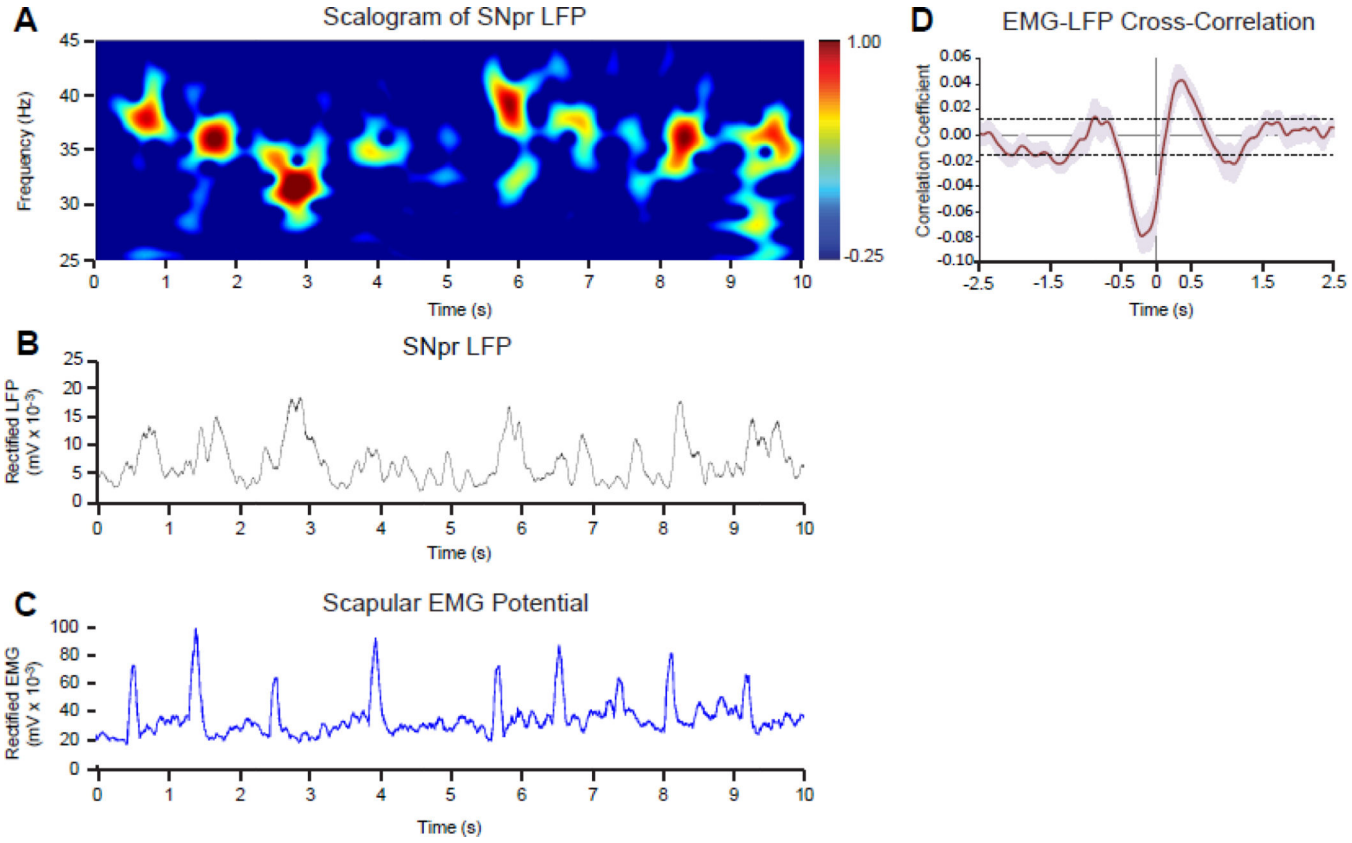

Figure 4.

Modulation of 25–40 Hz LFP power and EMG amplitude during treadmill walking. **A:** Wavelet-based scalogram shows a time-frequency representation of LFP power in the SNpr over a ten second epoch of treadmill walking. **B:** Line graph depicts amplitude of the rectified 25–40 Hz LFP from the same epoch as in A and **C. C:** Line graph shows EMG amplitude from the scapular EMG electrode contralateral to the lesioned hemisphere during the same epoch as in A and B. The treadmill speed during this epoch allowed the rat to walk consistently, stepping with the forelimb approximately once every 1.5 s. **D:** EMG-LFP cross-correlation (see Methods) shows notable movement-related modulation of the amplitude of 25–40 Hz SNpr LFP oscillatory activity in the dopamine-deprived hemisphere during walking. Data are presented as mean correlation coefficient averaged in 5 rats ±SEM (pink). Dotted lines represent ±3 SD of the mean values between −2.0 to −1.5 and 1.5 to 2.0 s, indicating significant modulation of LFP beta range oscillations in dopamine-depleted hemisphere by the stepping rhythm during walking.

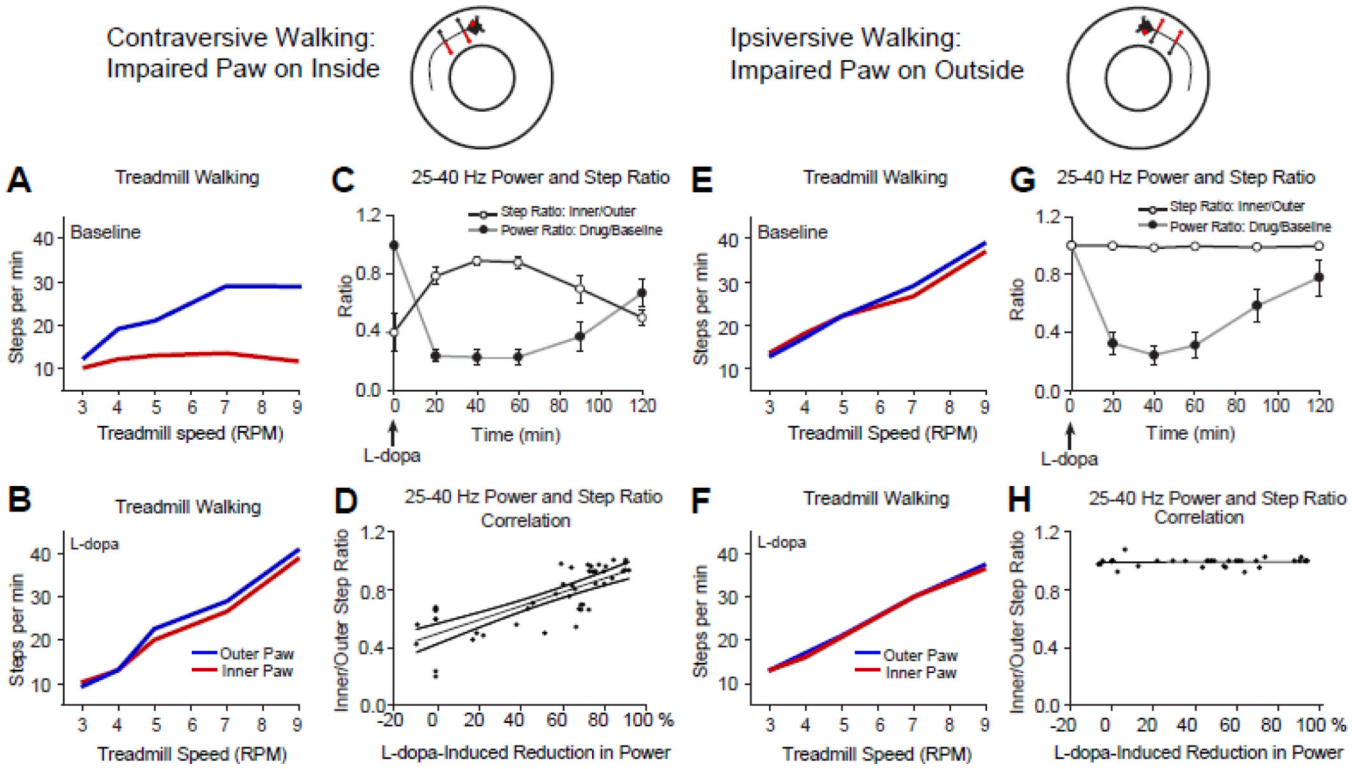

Figure 5.

The effect of treatment with L-dopa on 25–40 SNpr LFP power and gait during walking in the circular treadmill. Cartoons above the plots show the relationship between the direction of walking and the orientation of the affected paws (red) in the circular treadmill with respect to the dopamine cell-lesioned hemisphere (red dot). **A, B, E, F:** Line graphs show step counts for impaired (red, contralateral to lesion) and non-impaired (blue, ipsilateral to lesion) hind paws during contraversive (A, B) and ipsiversive (E, F) walking over a range of treadmill speeds. During contraversive walking (A, impaired paws on the inside of the track) the rat shows unbalanced stepping and progress in walking is disrupted. When the rat is walking ipsiversive to the lesion (E, impaired paws on the outside of the track) the rat is able to walk at a steady pace. L-dopa administration (5 mg/kg) improves stepping during contraversive walking (B), and gait becomes similar to baseline ipsiversive walking (E). **C, G:** Time-dependent reduction in 25–40 Hz range LFP power and associated improvement in treadmill walking (5 and 9 RPM) following L-dopa administration (n=4). Step ratios (number of steps by the inner limb vs. outer limb, black line) and power ratios (drug vs baseline beta/low gamma range LFP power, gray lines) are plotted vs. time after L-dopa treatment for contraversive (C) and ipsiversive (G) walking. After treatment with L-dopa, stepping ratios approach 1 as the rat walks more steadily in the contraversive direction (C) in conjunction with a reduction in beta power. L-dopa treatment does not affect step count ratios in G as the rat is able to walk effectively in the ipsiversive direction in the absence of treatment. **D, H:** Scatter plots depict percent change in the 25–40 Hz range LFP power vs ratio-based motor scores during walking in the circular treadmill following treatment with L-dopa, as shown in C and G. Improvements in stepping (ratios approaching 1) correlate with reduction in SNpr LFP power in the lesioned hemisphere during contraversive walking

following L-dopa treatment (D; Pearson coefficient, r=0.781, p<0.001). There is no correlation between reduction in SNpr LFP power following L-dopa treatment and step ratios during ipsiversive walking (H; Pearson coefficient r=0.075, p>0.05).

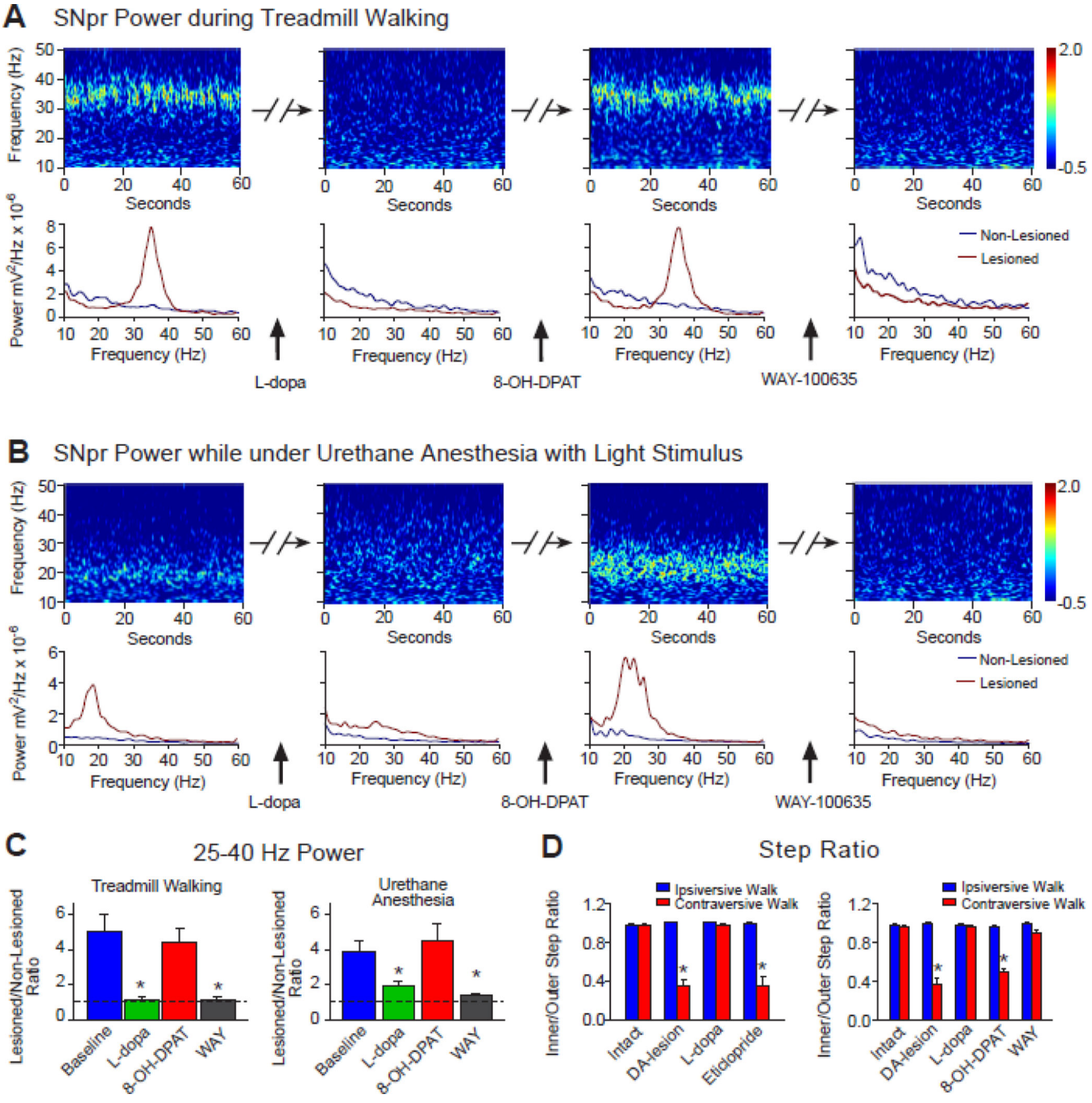

Figure 6.

Effect of a therapeutic dose of L-dopa (5 mg/kg) in rats with unilateral dopamine cell lesions on 25–40 Hz SNpr LFP power during ipsiversive walking and in anesthetized rats, reversal by the 5HT1A agonist 8-OH-DPAT, and step ratio during ipsiversive and contraversive walking. **A–B:** Representative wavelet-based scalograms with corresponding FFT-based power spectra below, showing LFP power during 4 series of consecutive recordings. A) Scalograms show LFP power during baseline ipsiversive treadmill walking, 20 min after L-dopa (5mg/kg), 5 min after subsequent administration of 8-OH-DPAT (0.2 mg/kg, 40 min

after L-dopa) and 3–5 min following injection of the 5HT1A antagonist WAY-100635 (0.3 mg/kg, 20 min after 8-OH-DPAT). B) The same drug treatment protocol as in A administered to a rat anesthetized with urethane (1 g/kg). Recordings were performed during periods of mild sensory stimulation as described in methods (n=5). **C:** Bar graphs represent mean ratios of 25–40 Hz SNpr LFP power in dopamine cell-lesioned hemisphere relative to non-lesioned hemisphere before and after treatment with drugs as in A during ipsiversive walking (left graph, n=7) and ratios of 15–30 Hz LFP power as in B in rats under urethane +SS (right graph, n=5). * $p<0.001$ compared to baseline and 8-OH-DPAT in awake rats (1-way RM ANOVA) and $p<0.04$ compared to baseline and 8-OH-DPAT in anesthetized rats (1-way RM ANOVA). Dotted line, representing a ratio of 1, indicates equal power in lesioned and non-lesioned hemispheres. **D:** Bar graphs represent step count ratios for the affected vs. unaffected hind limbs during ipsiversive (blue) and contraversive (red) walking at 9 RPM in the same rats before 6-OHDA lesion (intact) and on 21–23 days post-lesion, in control conditions and after L-dopa treatment. In left panel, rats were sequentially treated with L-dopa (5 mg/kg) and the D2 antagonist eticlopride (0.2 mg/kg, 40–60 min after L-dopa, N=5), and in right panel, rats were subsequently treated with 8-OH-DPAT followed by WAY-100635 (n=7)1, as shown in A. Note that increases in step ratios during contraversive walking after L-dopa treatment are reversed by both 8-OH-DPAT and eticlopride treatments. * $p<0.001$ compared to ipsiversive walking during the same conditions/drug treatment (2-way RM ANOVA). Impairment in gait during contraversive walking is associated with synchronization of LFP activity in the 25–40 Hz frequency range in the dopamine cell-lesioned hemisphere similar to that seen when rats are walking in ipsilateral direction.

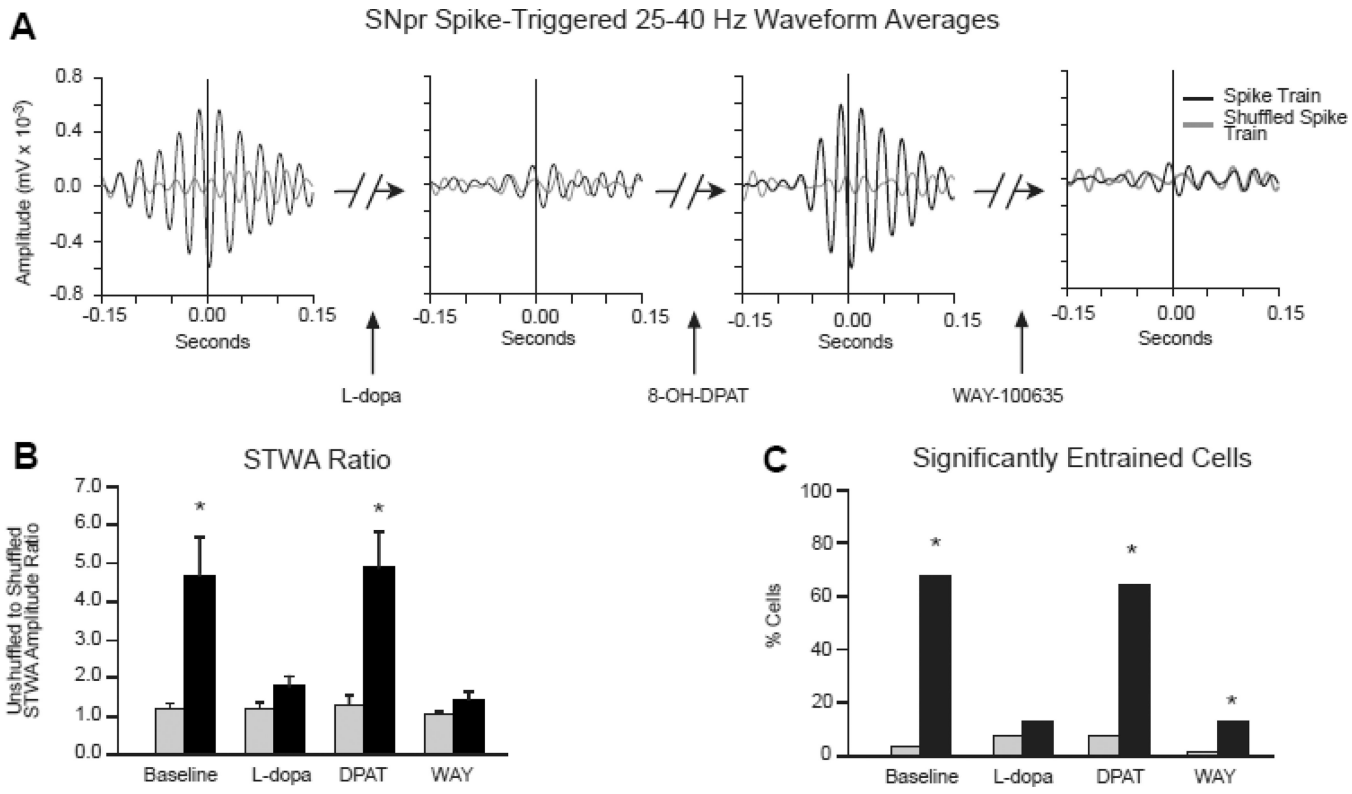

Figure 7.

The effect of L-dopa, 8-OH-DPAT and WAY-100635 treatments on phase-locking of SNpr spiking to 25–40 Hz LFP activity in dopamine cell-lesioned and non-lesioned hemispheres. **A:** Representative examples of spike-triggered LFP waveform averages (STWA) for a typical SNpr spike train in the lesioned hemisphere paired with simultaneously recorded SNpr LFP, band-pass filtered at 25–40 Hz. During treadmill walking, the STWA of the SNpr cell shows strong phase locking at ~90°, toward the trough of the SNpr LFP. L-dopa administration dramatically reduced phase-locking of the SNpr spikes, subsequent treatment with 8-OH-DPAT restored the spike-LFP synchronization and finally, treatment with WAY-100635 again reduced synchronization. Black line: unshuffled spike train; gray line: shuffled spike train. **B:** Bar graphs show the ratio of STWA-based peak-to-trough amplitudes of unshuffled vs. shuffled spike trains (see Methods) reflecting SNpr Spike-LFP synchronization in the dopamine cell lesioned hemisphere (black bars) and non-lesioned hemisphere (grey bars) before and after subsequent treatment with L-dopa, 8-OH-DPAT and WAY-100635. Dashed line represents a ratio of 1, indicating that STWA peak-to-trough amplitudes from shuffled and unshuffled spike trains are equal. Note the reduction in spike-LFP synchronization after L-dopa treatment, recovery following the 8-OH-DPAT and subsequent reduction by WAY-100635. * differences in mean STWA peak-to-trough amplitude ratios in the dopamine lesioned hemisphere (31 cells, 7 rats) relative to the non-lesioned hemisphere (25 cells, 7 rats) showing greater phase-locking of spikes with LFP in the dopamine-depleted hemisphere in baseline and after treatment with 8-OH-DPAT (2-way RM ANOVA, $p<0.001$). **C:** Bar graphs show the proportion of spike trains with spike timing significantly correlated to locally recorded LFPs in the 25–40 Hz range during walking (see

Methods) before and after subsequent treatment with L-dopa, 8-OH-DPAT and WAY-100635. *p<0.001 compared to percent correlated spike train in the non-lesioned hemisphere in matching conditions (Chi-squared test).